US 20030129085A1

(19) **United States**

(12) **Patent Application Publication** (10) **Pub. No.: US 2003/0129085 A1**

Suslick et al. (43) **Pub. Date: Jul. 10, 2003**

(54) **SILOXY PORPYHRINS AND METAL COMPLEXES THEREOF**

(75) Inventors: **Kenneth S. Suslick**, Champaign, IL (US); **Neal A. Rakow**, Champaign, IL (US); **Avijit Sen**, Urbana, IL (US)

Correspondence Address:
BANNER & WITCOFF, LTD.
TEN SOUTH WACKER DRIVE
SUITE 3000
CHICAGO, IL 60606 (US)

(73) Assignee: **Board of Trustees of the University of Illinois**, Champaign, IL (US)

(21) Appl. No.: **10/278,421**

(22) Filed: **Oct. 23, 2002**

Related U.S. Application Data

(60) Division of application No. 09/705,329, filed on Nov. 3, 2000, now Pat. No. 6,495,102, which is a continuation-in-part of application No. 09/532,125, filed on Mar. 21, 2000, now Pat. No. 6,368,558.

Publication Classification

(51) **Int. Cl.**[7] **G01N 21/00**

(52) **U.S. Cl.** **422/55**; 422/68.1; 422/82.05; 422/83; 422/85; 436/164; 436/172

(57) **ABSTRACT**

The present invention involves an artificial nose having an array comprising at least a first dye and a second dye in combination and having a distinct spectral response to an analyte. In one embodiment, the first and second dyes are from the group comprising porphyrin, chlorin, chlorophyll, phthalocyanine, or salen. In a further embodiment, the first and second dyes are metalloporphyrins. The present invention is particularly useful in detecting metal ligating vapors. Further, the array of the present invention can be connected to a wavelength sensitive light detecting device.

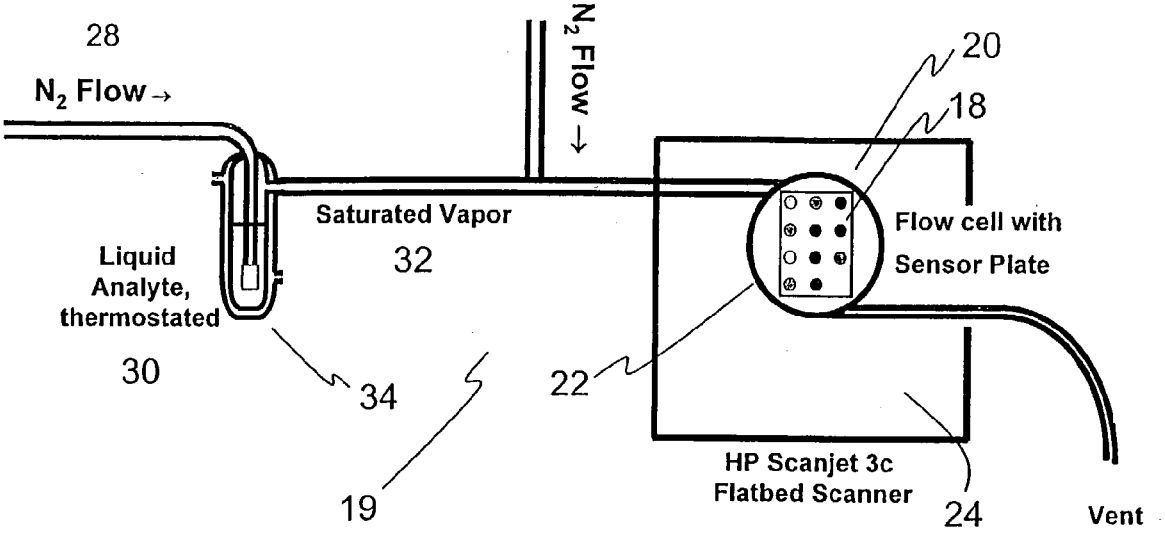

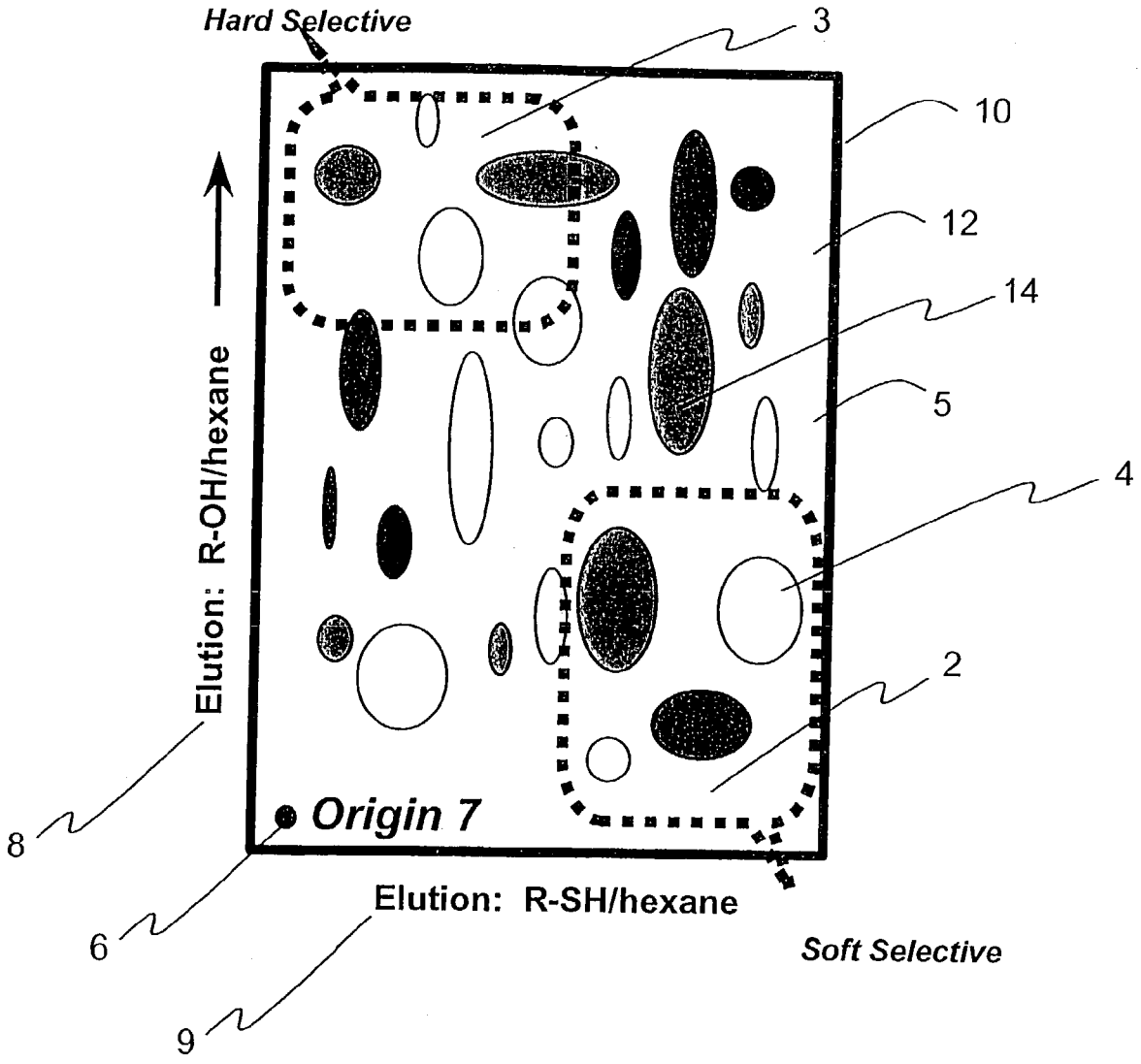
Hard Selective
3
10
12
14
5
4
2
Elution: R-OH/hexane
8
Origin 7
6
Elution: R-SH/hexane
9
Soft Selective

FIG. 1

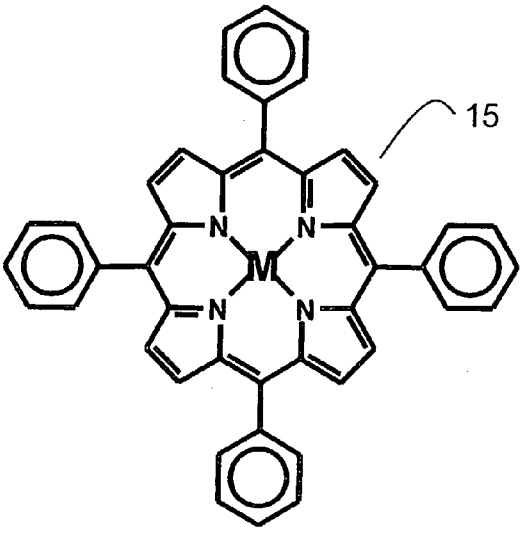

M(TPP)

Metal	Z/r Ratio ($Å^{-1}$)
Sn^{4+}	5.80
Co^{3+}	5.50
Cr^{3+}	4.88
Mn^{3+}	4.65
Fe^{3+}	4.65
Co^{2+}	3.08
Cu^{2+}	2.74
Ru^{2+}	2.71
Zn^{2+}	2.70
Ag^{2+}	2.13

FIG. 2A

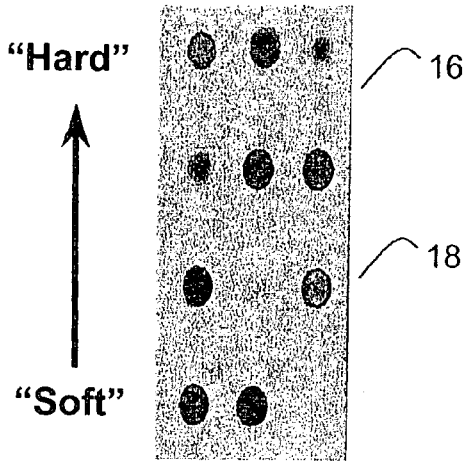

Sn^{4+} Co^{3+} Cr^{3+}

Mn^{3+} Fe^{3+} Co^{2+}

Cu^{2+} Ru^{2+} Zn^{2+}

Ag^{2+} $2H^{+}$
(FB)

FIG. 2B

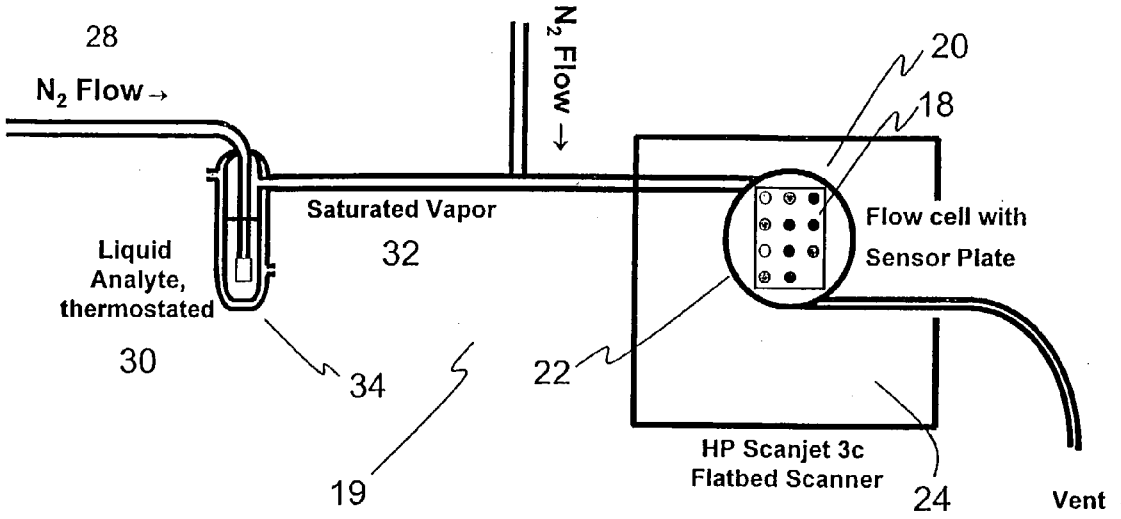
28
N_2 Flow →
N_2 Flow →
20
18
Saturated Vapor
32
Liquid
Analyte,
thermostated
30
34
22
Flow cell with
Sensor Plate
19
HP Scanjet 3c
Flatbed Scanner
24
Vent

FIG. 3A

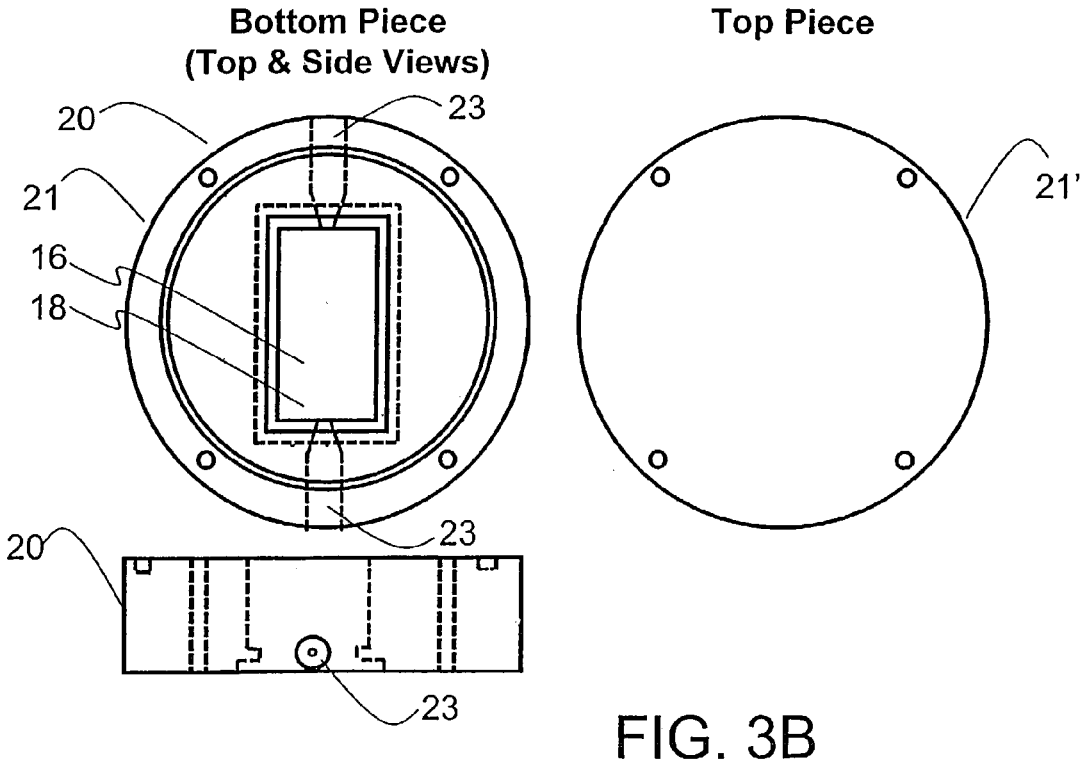
Bottom Piece
(Top & Side Views)
Top Piece
20
23
21
16
18
21'
20
23
23

FIG. 3B

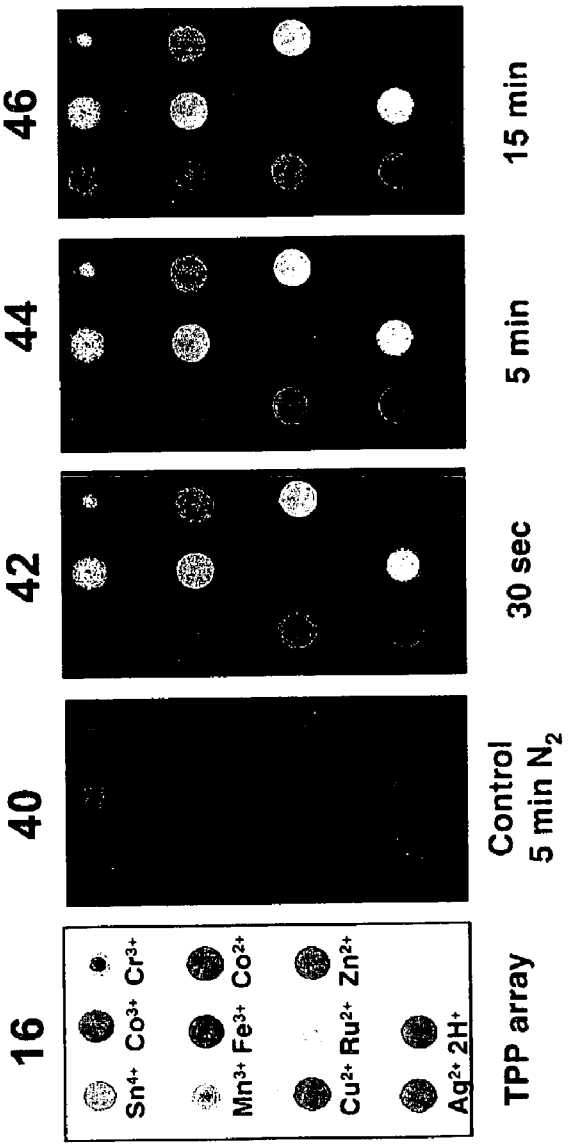
16
40
42
44
46
TPP array
Control
5 min N_2
30 sec
5 min
15 min
Sn^{4+} Co^{3+} Cr^{3+}
Mn^{3+} Fe^{3+} Co^{2+}
Cu^{2+} Ru^{2+} Zn^{2+}
Ag^{2+} $2H^{+}$

FIG. 4

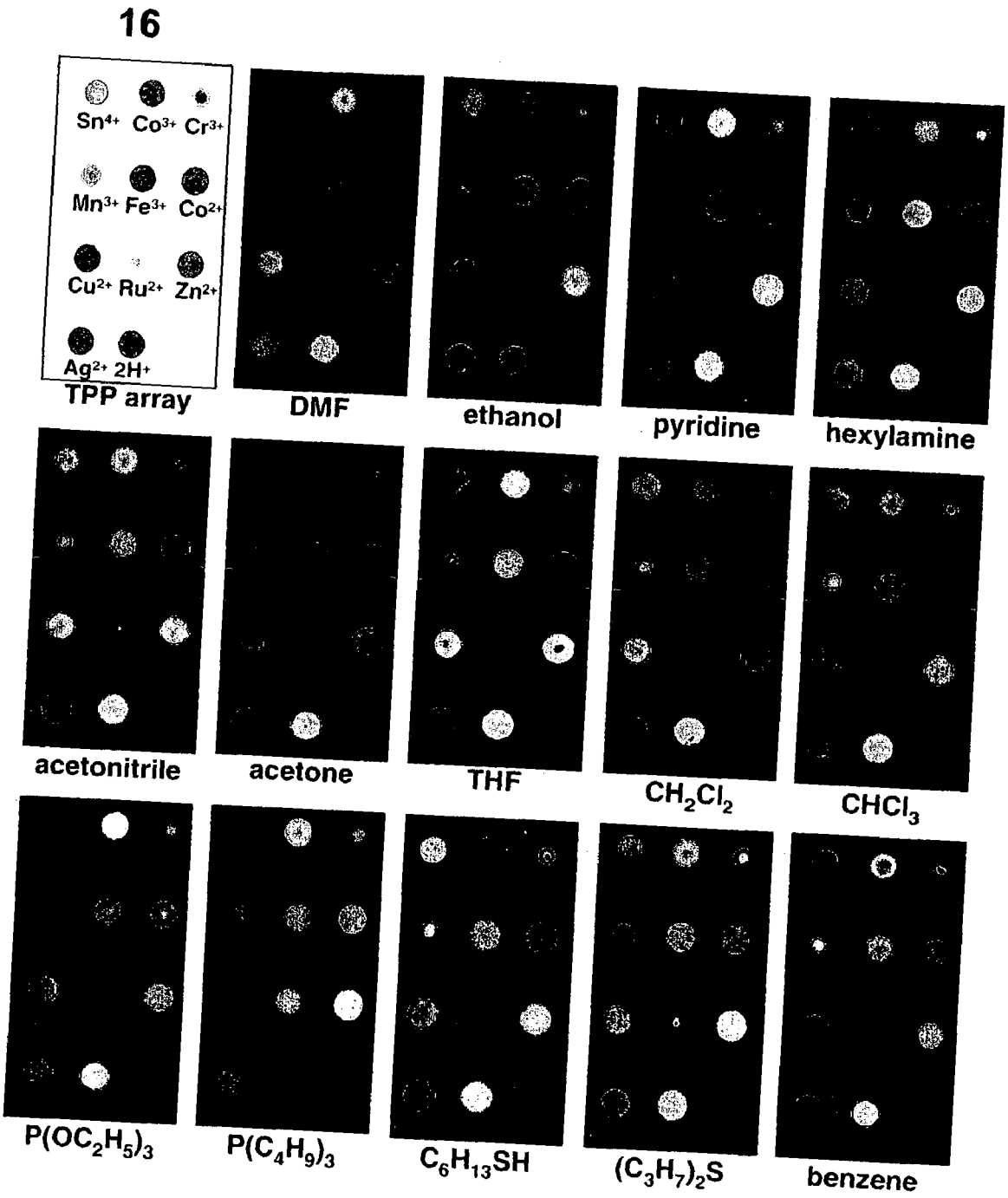
16
Sn4+ Co3+ Cr3+
Mn3+ Fe3+ Co2+
Cu2+ Ru2+ Zn2+
Ag2+ 2H+
TPP array
DMF
ethanol
pyridine
hexylamine
acetonitrile
acetone
THF
CH2Cl2
CHCl3
P(OC2H5)3
P(C4H9)3
C6H13SH
(C3H7)2S
benzene

FIG. 5

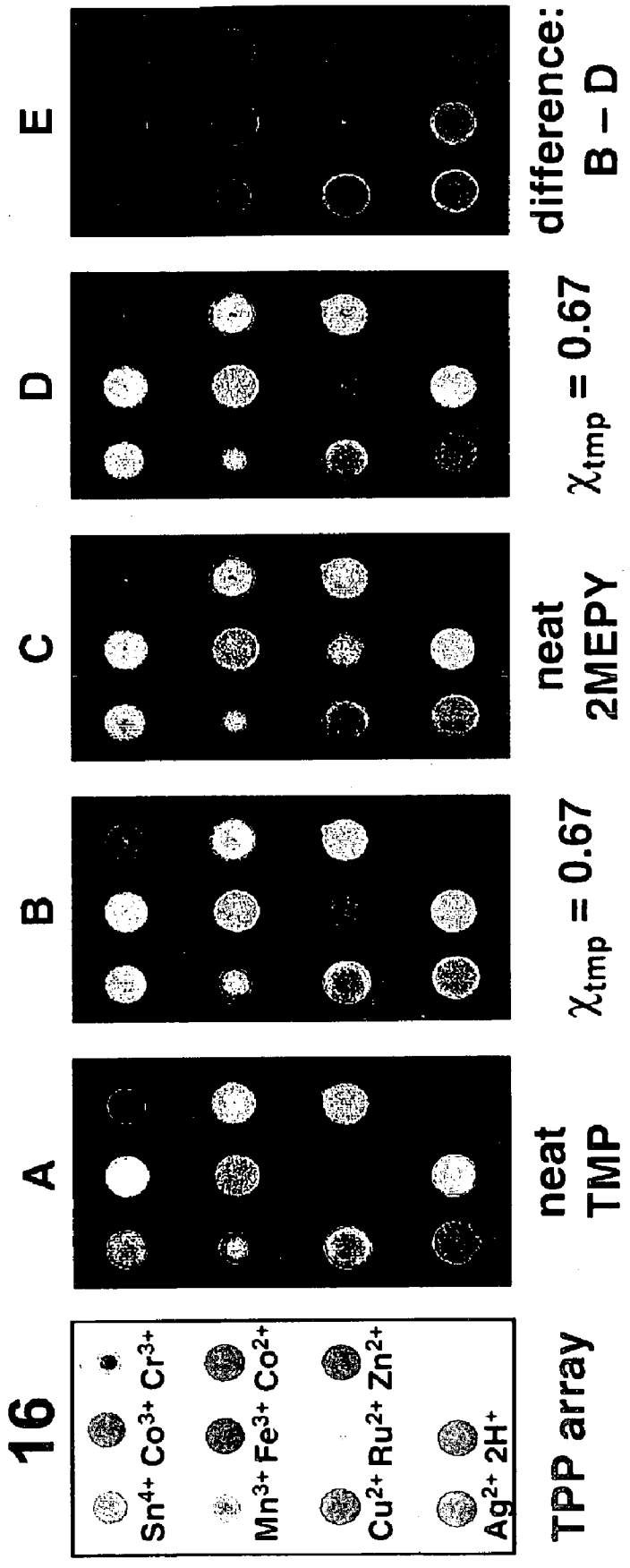
16
A
B
C
D
E
Sn^{4+} Co^{3+} Cr^{3+}
Mn^{3+} Fe^{3+} Co^{2+}
Cu^{2+} Ru^{2+} Zn^{2+}
Ag^{2+} $2H^{+}$
TPP array
neat TMP
χ_{tmp} = 0.67
neat 2MEPY
χ_{tmp} = 0.67
difference: B – D

FIG. 6

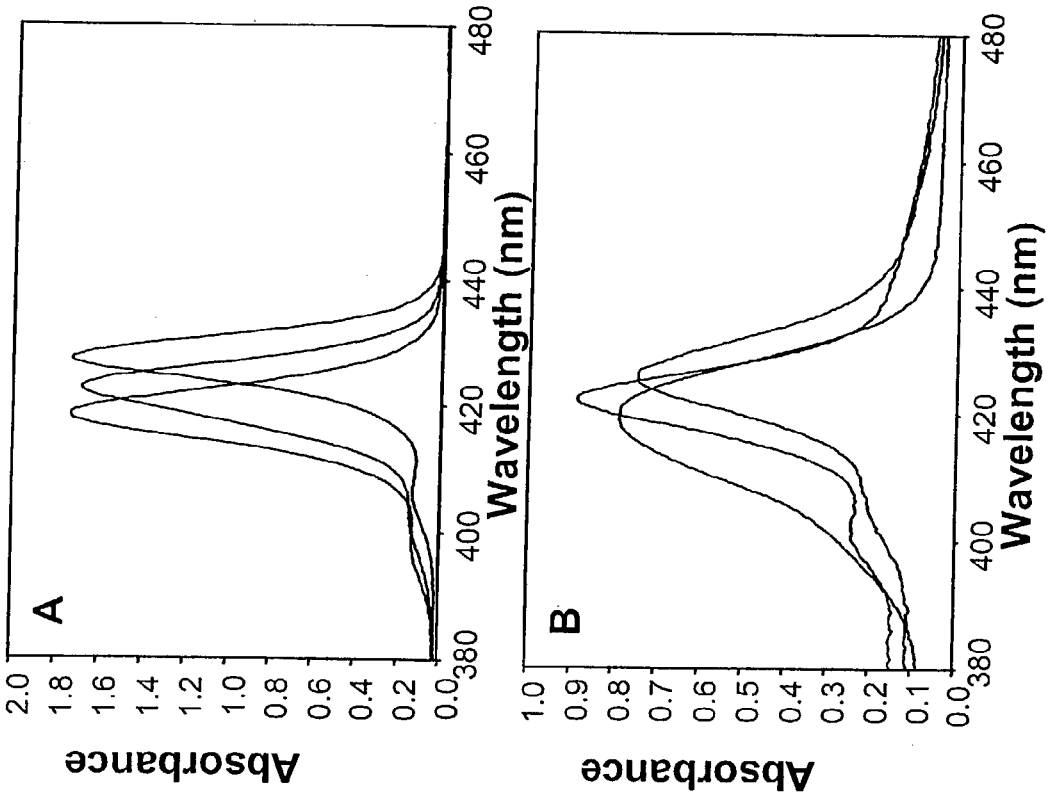
A
B
Absorbance
Wavelength (nm)
2.0
1.8
1.6
1.4
1.2
1.0
0.8
0.6
0.4
0.2
0.0
1.0
0.9
0.8
0.7
0.6
0.5
0.4
0.3
0.2
0.1
0.0
380
400
420
440
460
480

FIG. 7

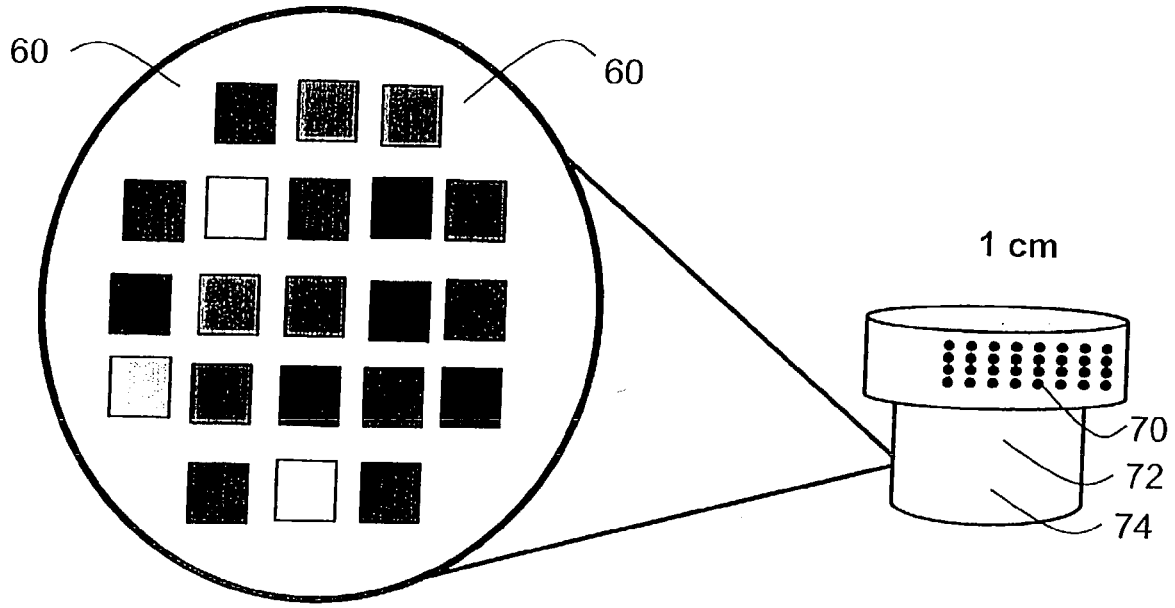

FIG. 8

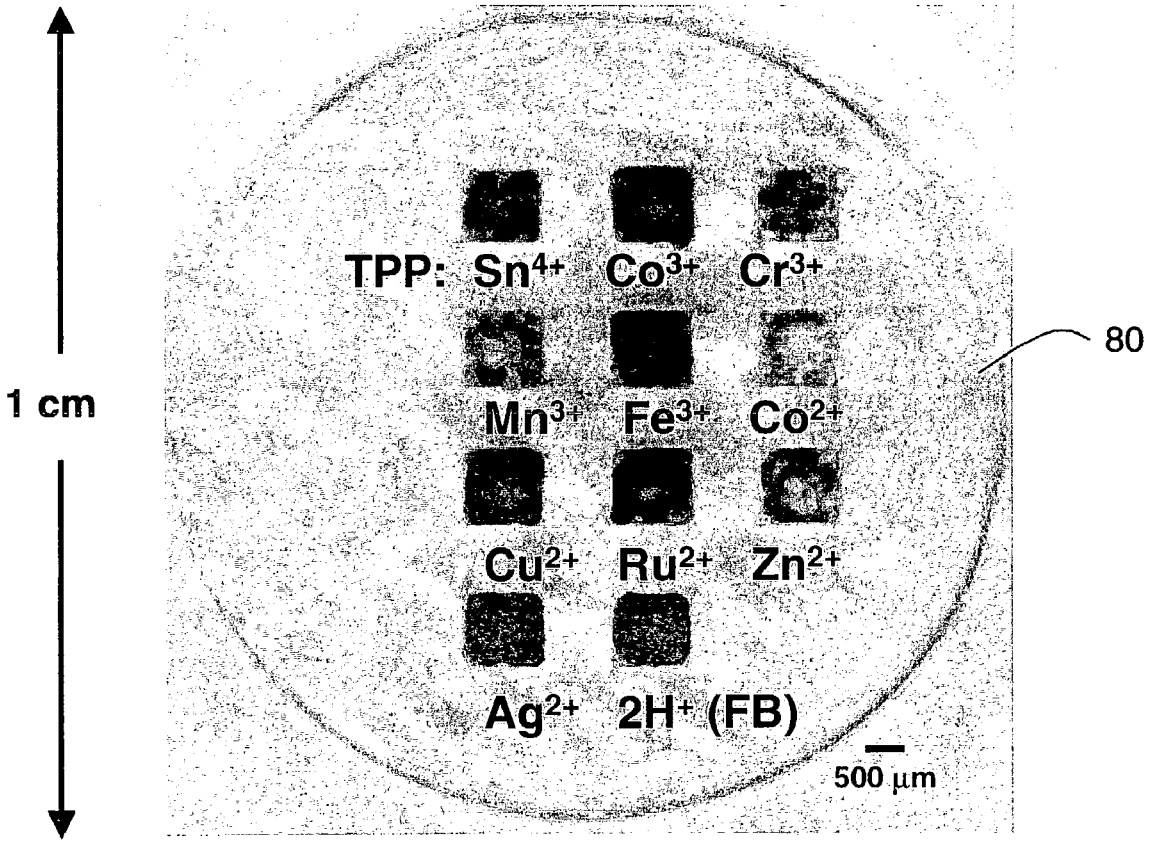

FIG. 9

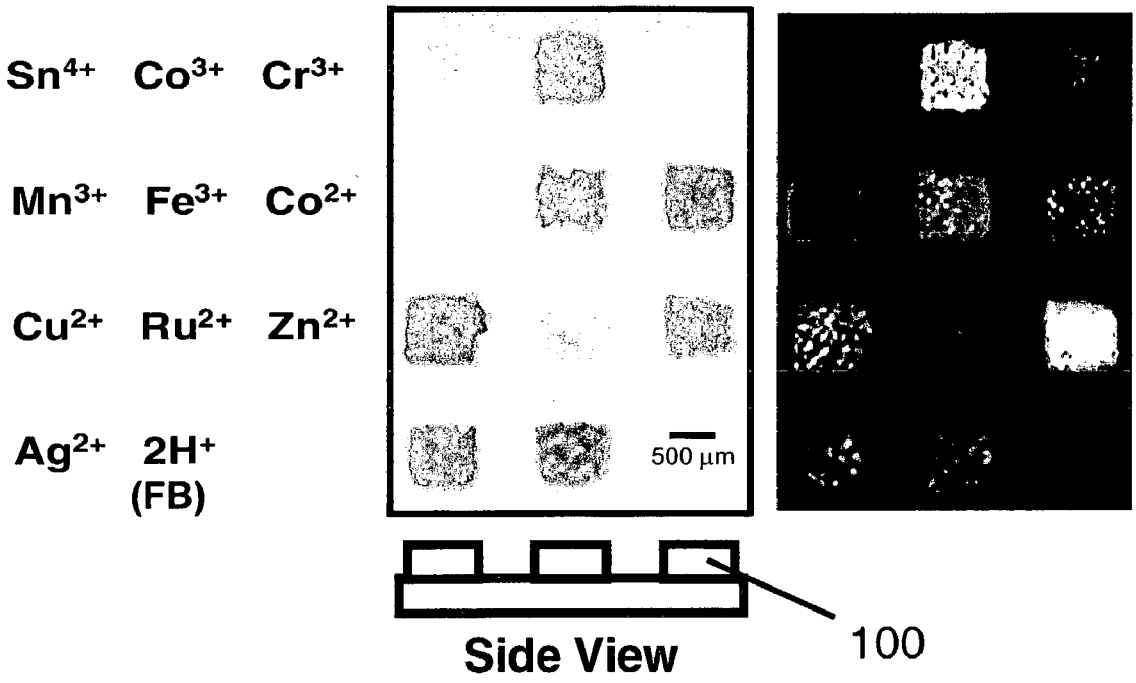
Sn^{4+} Co^{3+} Cr^{3+}
Mn^{3+} Fe^{3+} Co^{2+}
Cu^{2+} Ru^{2+} Zn^{2+}
Ag^{2+} $2H^{+}$ (FB)
500 µm
Side View
100

FIG. 10

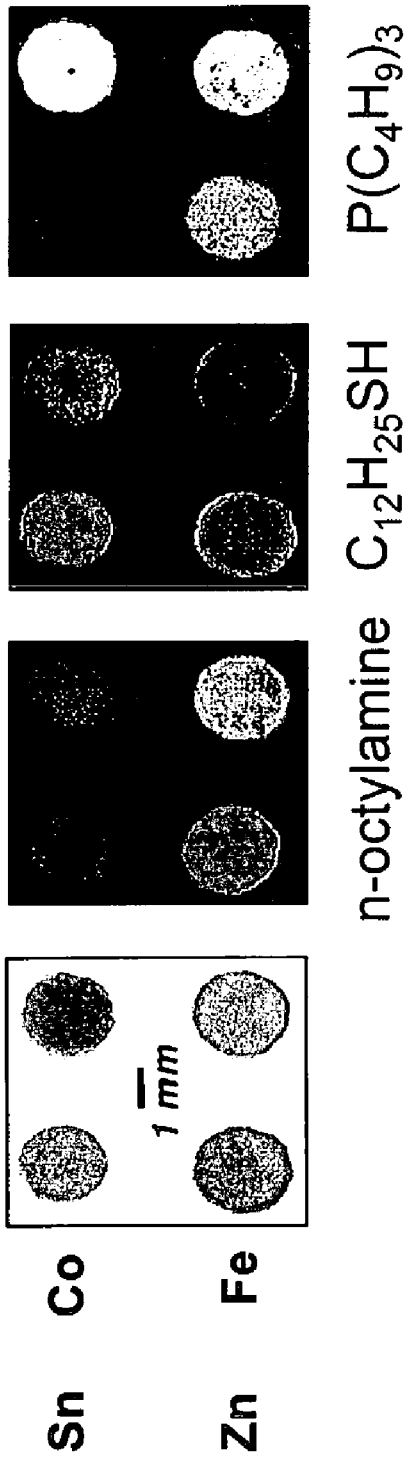

FIG. 11

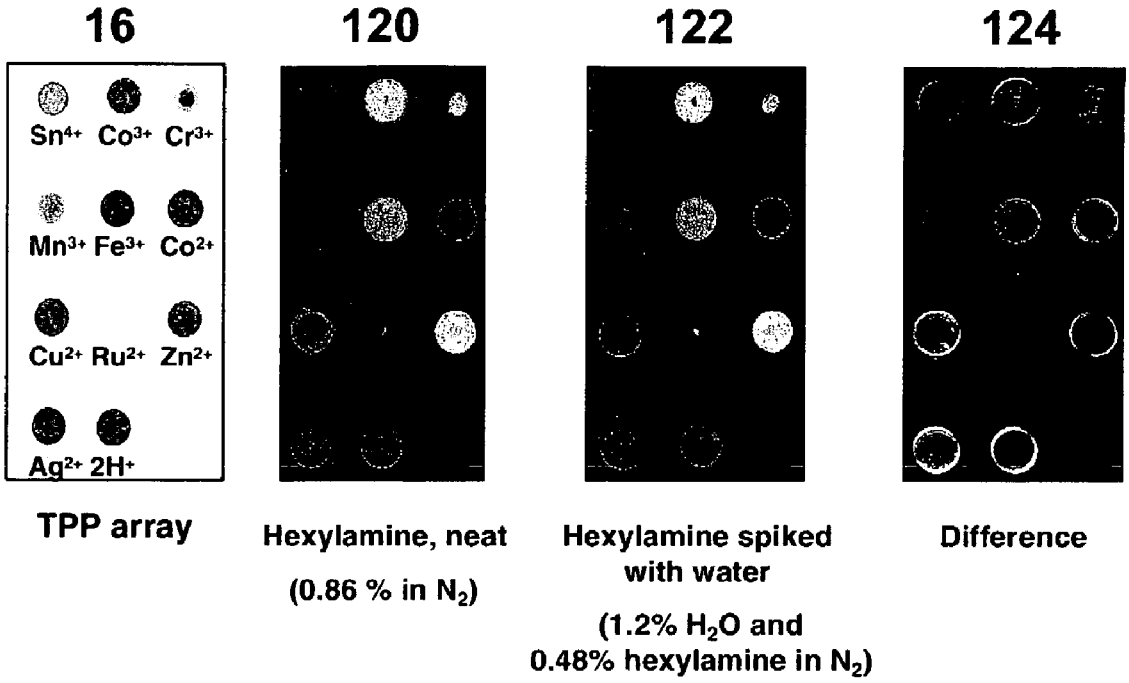
16
120
122
124
Sn4+ Co3+ Cr3+
Mn3+ Fe3+ Co2+
Cu2+ Ru2+ Zn2+
Ag2+ 2H+
TPP array
Hexylamine, neat
(0.86 % in N2)
Hexylamine spiked with water
(1.2% H2O and 0.48% hexylamine in N2)
Difference

FIG. 12

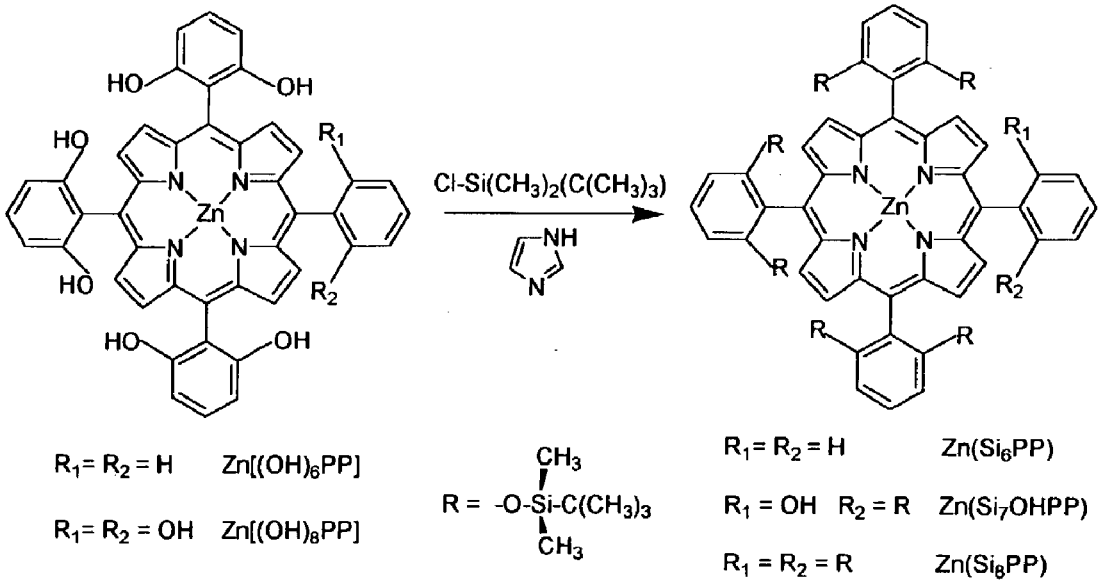
HO
OH
HO
HO
OH
R1
R2
N
N
N
N
Zn
Cl-Si(CH3)2(C(CH3)3)
NH
N
R
R
R
R
R
R
R1
R2
R1= R2 = H Zn[(OH)6PP]
R1= R2 = OH Zn[(OH)8PP]
R = -O-Si-C(CH3)3
CH3
CH3
R1= R2 = H Zn(Si6PP)
R1 = OH R2 = R Zn(Si7OHPP)
R1 = R2 = R Zn(Si8PP)

Figure 13

Figure 14a

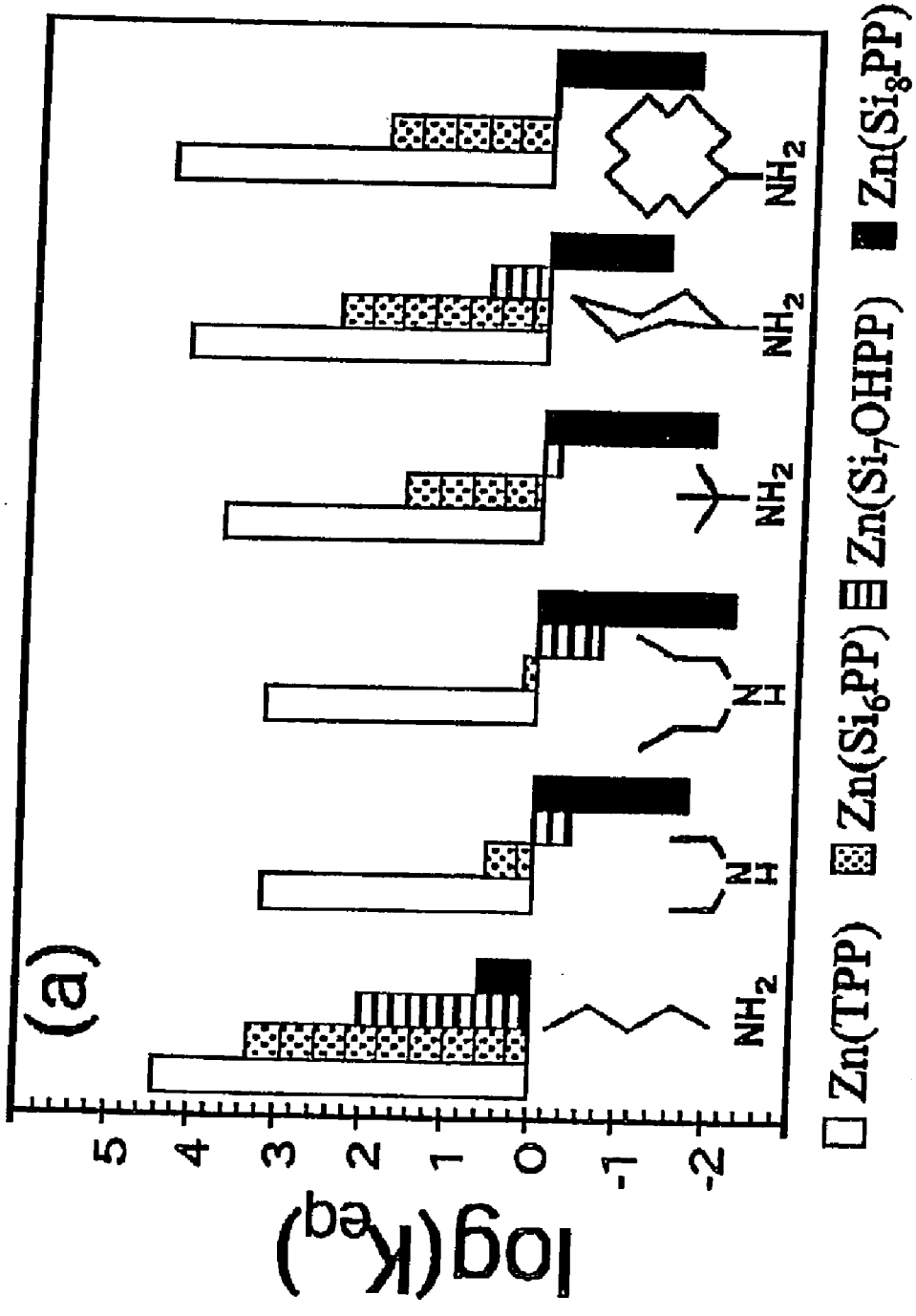
(a)
log(K_eq)
5
4
3
2
1
0
-1
-2
NH2
NH2
NH2
NH
NH
NH2
Zn(TPP)
Zn(Si6PP)
Zn(Si7OHPP)
Zn(Si8PP)

Figure 14b

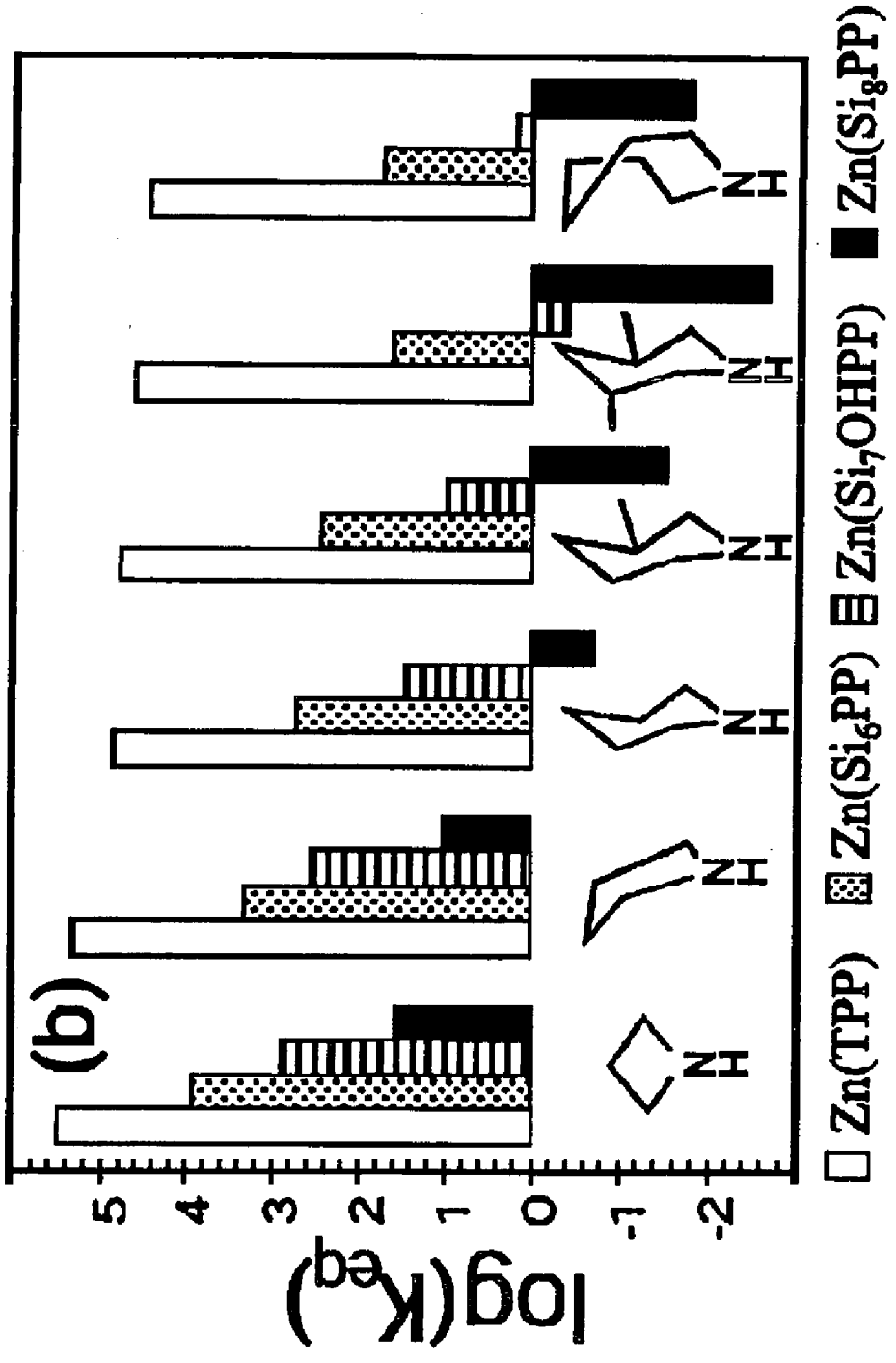

Figure 14c

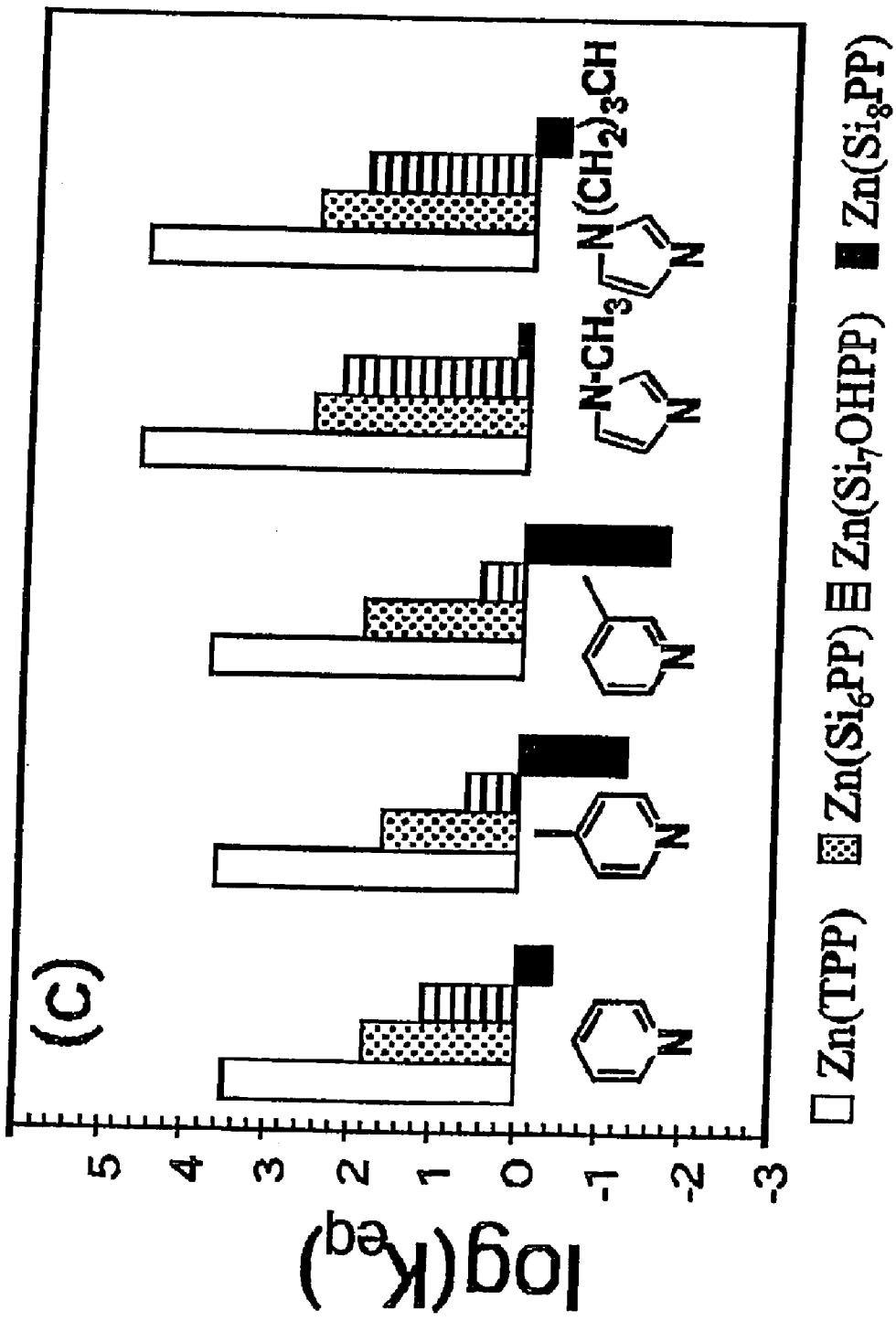
(C)
log(K_eq)
5
4
3
2
1
0
-1
-2
-3
N-CH3
N(CH2)3CH
Zn(TPP)
Zn(Si4PP)
Zn(Si7OHPP)
Zn(Si8PP)

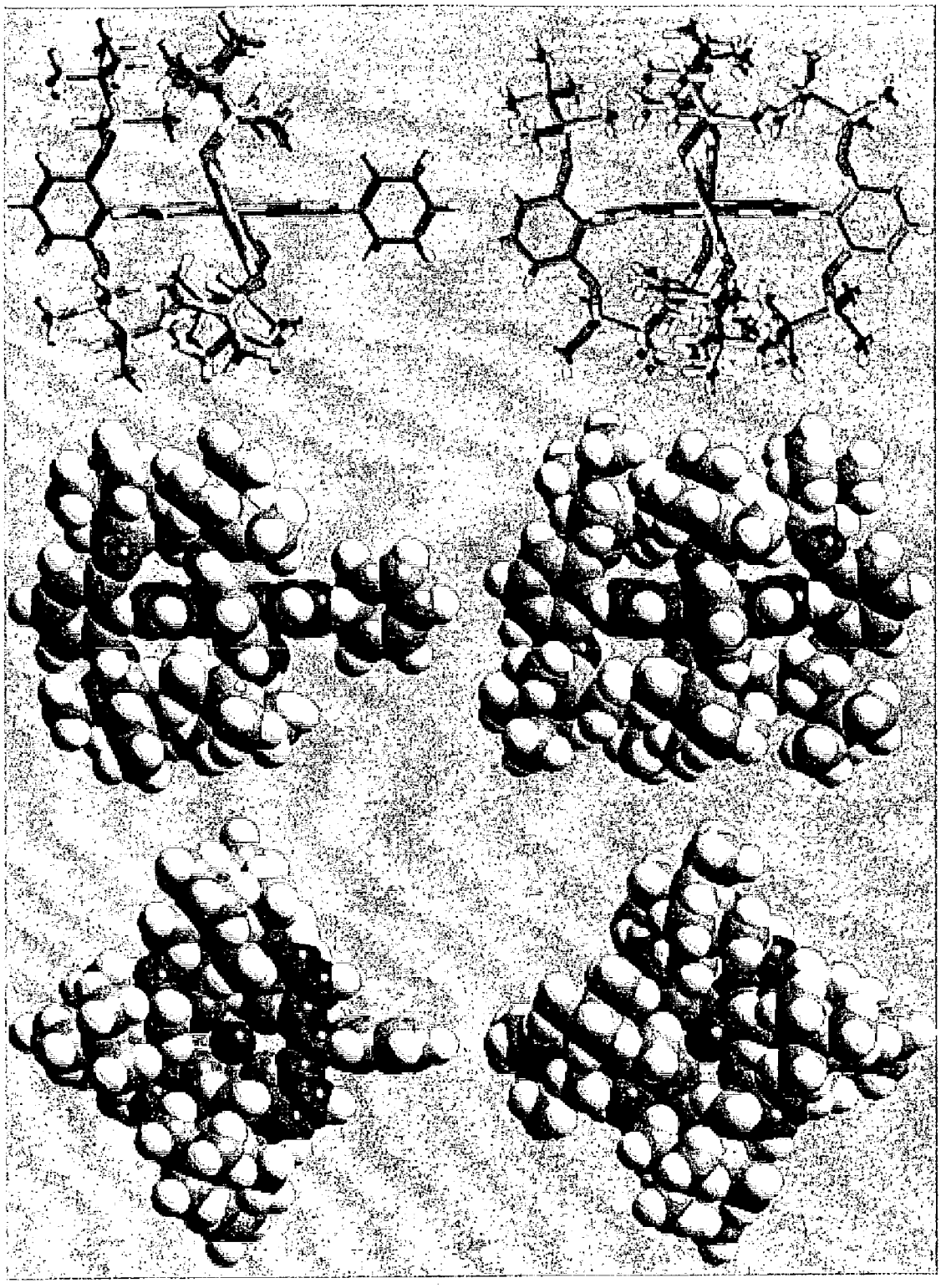

FIG. 15

SILOXY PORPYHRINS AND METAL COMPLEXES THEREOF

CONTINUING APPLICATION DATA

[0001] This application is a divisional of U.S. application Ser. No. 09/705,329, filed on Nov. 3, 2000, which is a Continuation-in-Part of U.S. application Ser. No. 09/532,125, filed on Mar. 21, 2000, now U.S. Pat. No. 6,638,558.

[0002] This invention was made with Government support under Contract Nos. HL25934 awarded by the National Institutes of Health & Contract No. DAAG55-97-1-2211 awarded by the Department of the Army. The Government has certain rights in the invention.

FIELD OF THE INVENTION

[0003] The present invention relates to methods and apparatus for artificial olfaction, e.g., artificial noses, for the detection of odorants by a visual display.

BACKGROUND OF THE INVENTION

[0004] There is a great need for olfactory or vapor-selective detectors (i.e., "artificial noses") in a wide variety of applications. For example, there is a need for artificial noses that can detect low levels of odorants and/or where odorants may be harmful to humans, animals or plants. Artificial noses that can detect many different chemicals are desirable for personal dosimeters in order to detect the type and amount of odorants exposed to a human, the presence of chemical poisons or toxins, the spoilage in foods, the presence of flavorings, or the presence of vapor emitting items, such as plant materials, fruits and vegetables, e.g., at customs portals.

[0005] Conventional artificial noses have severe limitations and disadvantages and are not considered generally useful for such purposes. Limitations and disadvantages of conventional artificial noses include their need for extensive signal transduction hardware, and their inability to selectively target metal-coordinating vapors and toxins. In addition, artificial noses which incorporate mass sensitive signal transduction or polar polymers as sensor elements are susceptible to interference by water vapor. This limitation is significant in that it can cause variable response of the detector with changes ambient humidity. See F. L. Dickert, O. Hayden, Zenkel, M. E. *Anal. Chem.* 71, 1338 (1999).

[0006] Initial work in the field of artificial noses was conducted by Wilkens and Hatman in 1964, though the bulk of research done in this area has been carried out since the early 1980's. See, e.g., W. F. Wilkens, A. D. Hatman. *Ann. NY Acad. Sci.,* 116, 608 (1964); K. Pursaud, G. H. Dodd. *Nature,* 299, 352-355 (1982); and J. W. Gardner, P. N. Bartlett. *Sensors and Actuators B,* 18-19, 211-220 (1994).

[0007] Vapor-selective detectors or "artificial noses" are typically based upon the production of an interpretable signal or display upon exposure to a vapor emitting substance or odorant (hereinafter sometimes referred to as an "analyte"). More specifically, typical artificial noses are based upon selective chemical binding or an interface between a detecting compound of the artificial nose and an analyte or odorant, and then transforming that chemical binding into a signal or display, i.e., signal transduction.

[0008] Polymer arrays having a single dye have been used for artificial noses. That is, a series of chemically-diverse polymers or polymer blends are chosen so that their composite response distinguishes a given odorant or analyte from others. Examples of polymer array vapor detectors, including conductive polymer and conductive polymer/carbon black composites, are discussed in: M. S. Freund, N. S. Lewis, *Proc. Natl. Acad. Sci. USA* 92,2652-2656 (1995); B. J. Doleman, R. D. Sanner, E. J. Severin, R. H. Grubbs, N. S. Lewis, *Anal. Chem.* 70, 2560-2564 (1998); T. A. Dickinson, J. White, J. S. Kauer, D. R. Walt, *Nature* 382, 697-700 (1996)(polymer array with optical detection); A. E. Hoyt, A. J. Ricco, H. C. Yang, R. M. Crooks, *J. Am. Chem. Soc.* 117, 8672 (1995); and J. W. Grate, M. H. Abraham, *Sensors and Actuators B* 3, 85-111 (1991).

[0009] Other interface materials include functionalized self-assembled monolayers (SAM), metal oxides, and dendrimers. Signal transduction is commonly achieved with mass sensitive piezoelectric substrates, surface acoustic wave (SAW) transducers, or conductive materials. Optical transducers (based on absorbance or luminescence) have also been examined. Examples of metal oxide, SAM, and dendrimer-based detectors are discussed in J. W. Gardner, H. V. Shurmer, P. Corcoran, *Sensors and Actuators B* 4, 117-121 (1991); J. W. Gardner, H. V. Shurmer, T. T. Tan, *Sensors and Actuators B* 6, 71-75 (1992); and R. M. Crooks, A. J. Ricco, *Acc. Chem. Res.* 31, 219-227 (1998). These devices also use a single dye.

[0010] Techniques have also been developed using a metalloporphyrin for optical detection of a specific, single gas such as oxygen or ammonia, and for vapor detection by chemically interactive layers on quartz crystal microbalances. See A. E. Baron, J. D. S. Danielson, M. Gouterman, J. R. Wan, J. B. Callis, *Rev. Sci. Instrum.* 64, 3394-3402 (1993); J. Kavandi, et al., *Rev. Sci. Instrum.* 61, 3340-3347 (1990); W. Lee, et al., *J. Mater. Chem.* 3, 1031-1035 (1993); A. A. Vaughan, M. G. Baron, R. Narayanaswamy, *Anal Comm.* 33,393-396 (1996); J. A. J. Brunink, et al., *Anal. Chim. Acta* 325,53-64 (1996); C. Di Natale, et al., *Sensors and Actuators B* 44, 521-526 (1997); and C. Di Natale, et al., *Mat. Sci. Eng. C* 5, 209-215 (1998). However, these techniques either require extensive signal transduction hardware, or, as noted above, are limited to the detection of a specific, single gas. They are also subject to water vapor interference problems, as discussed previously.

[0011] While typical systems to date have demonstrated some success in chemical vapor detection and differentiation, these systems have focused on the detection of non-metal binding or non-metal ligating solvent vapors, such as arenes, halocarbons and ketones. Detection of metal-ligating vapors (such as amines, thiols, and phosphines) has been much less explored. Further, while some single porphyrin based sensors have been used for detection of a single strong acid, there is a need for sensor devices that will detect a wide variety of vapors.

[0012] To summarize, there are a number of limitations and drawbacks to typical artificial noses and single porphyrin based sensors. As noted above typical artificial noses are not designed for metal binding and metal ligating vapors, such as amines, thiols, and phosphines. Further, typical artificial noses require extensive signal transduction hardware, and are subject to interference from water vapor. As

noted above, single porphyrin based sensors have been used for detection of a single strong acid, but cannot detect a wide variety of vapors. Thus, there is a need for new artificial noses and methods that overcome these and other limitations of prior artificial noses and single porphyrin based sensors and methods.

SUMMARY OF THE INVENTION

[0013] The present invention comprises an array of dyes including at least a first dye and a second dye which in combination provide a spectral response distinct to an analyte or odorant. The dyes of the present invention produce a response in the spectrum range of about 200 nanometers to 2,000 nanometers, which includes the visible spectrum of light. It has now been discovered that an array of two or more dyes responds to a given ligating species with a unique color pattern spectrally and in a time dependent manner. Thus, dyes in the array of the present invention are capable of changing color in a distinct manner when exposed to any one analyte or odorant. The pattern of colors manifested by the multiple dyes is indicative of a specific or given analyte. In other words, the pattern of dye colors observed is indicative of a particular vapor or liquid species.

[0014] In a preferred embodiment, the dyes of the array are porphyrins In another preferred embodiment, the porphyrin dyes are metalloporphyrins. In a further preferred embodiment, the array will comprise ten to fifty distinct metalloporphyrins in combination. Metalloporphyrins are preferable dyes in the present invention because they can coordinate metal-ligating vapors through open axial coordination sites, and they produce large spectral shifts upon binding of or interaction with metal-ligating vapors. In addition, porphyrins, metalloporphyrins, and many dyes show significant color changes upon changes in the polarity of their environment; this so-called solvatochromic effect will give net color changes even in the absence of direct bonding between the vapor molecules and the metal ions. Thus, metalloporphyrins produce intense and distinctive changes in coloration upon ligand binding with metal ligating vapors.

[0015] The present invention provides a means for the detection or differentiation and quantitative measurement of a wide range of ligand vapors, such as amines, alcohols, and thiols. Further, the color data obtained using the arrays of the present innovation may be used to give a qualitative fingerprint of an analyte, or may be quantitatively analyzed to allow for automated pattern recognition and/or determination of analyte concentration. Because porphyrins also exhibit wavelength and intensity changes in their absorption bands with varying solvent polarity, weakly ligating vapors (e.g., arenes, halocarbons, or ketones) are also differentiable.

[0016] Diversity within the metalloporphyrin array may be obtained by variation of the parent porphyrin, the porphyrin metal center, or the peripheral porphyrin substituents. The parent porphyrin is also referred to as a free base ("FB") porphyrin, which has two central nitrogen atoms protonated (i.e., hydrogen cations bonded to two of the central pyrrole nitrogen atoms). A preferred parent porphyrin is depicted in **FIG. 2**A, with the substitution of a two hydrogen ion for the metal ion (depicted as "M") in the center of the porphyrin. In **FIG. 2**A, TTP stands for 5,10,15,20-tetraphenylporphyrinate(-2).

[0017] In accordance with the present invention, colorimetric difference maps can be generated by subtracting unexposed and exposed metalloporphyrin array images (obtained, for example, with a common flatbed scanner or inexpensive video or charge coupled device ("CCD") detector) with image analysis software. This eliminates the need for extensive and expensive signal transduction hardware associated with previous techniques (e.g., piezoelectric or semiconductor sensors). By simply differencing images of the array before and after exposure to analytes, the present invention provides unique color change signatures for the analytes, for both qualitative recognition and quantitative analysis.

[0018] Sensor plates which incorporate vapor sensitive combinations of dyes comprise an embodiment of the present invention which is economical, disposable, and can be utilized to provide qualitative and/or quantitative identification of an analyte. In accordance with the present invention, a catalog of arrays and the resultant visual pattern for each analyte can be coded and placed in a look-up table or book for future reference. Thus, the present invention includes a method of detecting an analyte comprising the steps of forming an array of at least a first dye and a second dye, subjecting the array to an analyte, inspecting the first and second dyes for a spectral response, and comparing the spectral response with a catalog of analyte spectral responses to identify the analyte.

[0019] Because sensing is based upon either covalent interaction (i.e., ligation) or non-covalent solvation interactions between the analyte and the porphyrin array, a broad spectrum of chemical species is differentiable. While long response times (e.g., about 45 minutes) are observed at low analyte concentrations of about 1 ppm with large reverse phase silica gel plates, use of impermeable solid supports (such as polymer- or glass-based micro-array plates) or of small (e.g., about 1 square cm.) substantially increases the low-level response to about 5 minutes.

[0020] Thus, it is an object of the present invention to provide methods and devices for artificial olfaction, vapor-selective detectors or artificial noses for a wide variety of applications. It is another object of the present invention to provide methods of detection and artificial noses that can detect low levels of odorants and/or where odorants may be harmful to living human, animal or plant cells. It is also an object of the present invention to provide methods of olfactory detection and artificial noses that can detect and quantify many different chemicals for dosimeters that can detect chemical poisons or toxins, that can detect spoilage in foods, that can detect flavorings and additives, and that can detect plant materials, e.g., fruits and vegetables.

[0021] Another object of the present invention is to provide for the detection of analytes using data analysis/pattern recognition techniques, including automated techniques.

BRIEF DESCRIPTION OF THE DRAWINGS

[0022] The file of this patent contains at least one drawing executed in color. Copies of this patent with color drawing(s) will be provided by the Patent and Trademark Office upon request and payment of the necessary fee.

[0023] **FIG. 1** illustrates an embodiment of the optical sensing plate of the present invention using a first elution in

the y axis and a second elution in the x axis of the plate. In this embodiment the first elution R—OH/hexane and the second elution is R—SH/hexane.

[0024] **FIG. 2A** illustrates an embodiment of the invention using metalloporphyrins as the sensing dyes.

[0025] FIG. 2B illustrates an embodiment of the invention using metalloporphyrins as the sensing dyes.

[0026] **FIG. 3A** illustrates a vapor exposure apparatus for demonstration of the present invention.

[0027] **FIG. 3B** illustrates a vapor exposure apparatus for demonstration of the present invention.

[0028] FIG. 4 illustrates the color change profile in a metalloporphyrin array of **FIG. 2** when used in the vapor exposure apparatus of **FIG. 3A** to detect n-butylamine. Metalloporphyrins were immobilized on reverse phase silica gel plates.

[0029] **FIG. 5** illustrates a comparison of color changes at saturation for a wide range of analytes. Each analyte was delivered to the array as a nitrogen stream saturated with the analyte vapor at 20° C. DMF stands for dimethylformamide; THF stands for tetrahydrofuran.

[0030] **FIG. 6** illustrates two component saturation responses of mixtures of 2-methylpyridine and trimethylphosphite. Vapor mixtures were obtained by mixing two analyte-saturated N_2 streams at variable flow ratios.

[0031] **FIG. 7** illustrates a comparison of Zn(TPP) spectral shifts upon exposure to ethanol and pyridine (py) in methylene chloride solution (A) and on the reverse phase support (B).

[0032] **FIG. 8** illustrates another embodiment of the present invention, and more particularly, an small array comprising microwells built into a wearable detector which also contains a portable light source and a light detector, such as a charge-coupled device (CCD) or photodiode array.

[0033] **FIG. 9** illustrates another embodiment of the present invention, and more particularly, a microwell porphyrin array wellplate constructed from polydimethylsiloxane (PDMS).

[0034] **FIG. 10** illustrates another embodiment of the present invention, and more particularly, a microplate containing machined teflon posts, upon which the porphyrin array is immobilized in a polymer matrix (polystyrene/dibutylphthalate).

[0035] **FIG. 11** illustrates another embodiment of the present invention, showing a microplate of the type shown in **FIG. 10**, consisting of a minimized array of four metalloporphyrins, showing the color profile changes for n-octylamine, dodecanethiol, and tri-n-butylphosphine, each at 1.8 ppm.

[0036] **FIG. 12** illustrates the immunity of the present invention to interference from water vapor.

[0037] **FIG. 13** illustrates the synthesis of siloxyl-substituted bis-pocket porphyrins in accordance with the present invention.

[0038] **FIGS. 14*a***, **14*b***, and **14*c*** illustrate differences in K_{eq} for various porphyrins.

[0039] **FIG. 15** illustrates molecular models of Zn(Si_6PP) (left column) and Zn(Si_8PP) (right column).

DETAILED DESCRIPTION OF THE PREFERRED EMBODIMENTS

[0040] Production of The Sensor Plate of the Present Invention A sensor plate **10** fabricated in accordance with the present invention is shown in **FIG. 1**. Sensor plate **10** comprises a two-dimensionally spatially resolved array **12** of various sensing elements or dyes **14** capable of changing color upon interaction (e.g., binding, pi-pi complexation, or polarity induced shifts in color). As shown in **FIG. 1, a** library of such dyes **14** can be given spatial resolution by two-dimensional chromatography or by direct deposition, including, but not limited to, ink-jet printing, micropipette spotting, screen printing, or stamping. In **FIG. 1**, metalloporphyrin mixture **6** is placed at origin **7**. Next, the metalloporphyrin mixture **6** is eluted through a silica gel or reversed-phase-silica gel **5** in sensor plate **10**, and the metalloporphyrins are spatially resolved from each other and immobilized in silica gel **5** as depicted by the oval and circular shapes **4** as shown in **FIG. 1**. Sensor plate **10** can be made from any suitable material or materials, including but not limited to, chromatography plates, paper, filter papers, porous membranes, or properly machined polymers, glasses, or metals.

[0041] **FIG. 1** also illustrates an embodiment of the optical sensing plate of the present invention using a first elution **8** in the y axis and a second elution **9** in the x axis of sensor plate **10**. In this embodiment, the first elution **8** is R—OH/hexane and the second elution **9** is R—SH/hexane. The order of the first and second elutions can be reversed. The first and second elutions are used to spatially resolve the metalloporphyrin mixture **6** in silica gel **5**. As shown in **FIG. 1**, the upper left hand quadrant **3** is characterized by metalloporphyrins that are "hard" selective, i.e., having a metal center having a high chemical hardness, i.e., a high charge density. As shown in **FIG. 1**, the lower right hand quadrant **2** is characterized by metalloporphyrins that are "soft" selective, i.e., having a metal center having a low chemical hardness, i.e., a low charge density. In accordance with the present invention, the array can be a spatially resolved collection of dyes, and more particularly a spatially resolved combinatorial family of dyes.

[0042] In accordance with the present invention, a porphyrin-metalloporphyrin sensor plate was prepared and then used to detect various odorants. More specifically, solutions of various metalated tetraphenylporphyrins in either methylene chloride or chlorobenzene were spotted in 1 μL aliquots onto two carbon ("C2", i.e, ethyl-capped) reverse phase silica thin layer chromatography plates (Product No. 4809-800, by Whatman, Inc., Clifton, N.J.) to yield the sensor array **16** seen in FIG. 2B. As shown in FIG. 2B and summarized in Table 1 below, the dyes have the following colors (the exact colors depend, among other things, upon scanner settings).

TABLE 1

(Summarizing Colors of Dyes in FIG. 2B)

Sn^{4+}—Green	Co^{3+}—Red	Cr^{3+}—Deep Green
Mn^{3+}—Green	Fe^{3+}—Dark Red	Co^{2+}—Red

TABLE 1-continued

(Summarizing Colors of Dyes in FIG. 2B)

Cu^{2+}—Red	Ru^{2+}—Light Yellow	Zn^{2+}—Greenish Red
Ag^{2+}—Red	$2H^{+}$ (Free Base "FB")—Red	

[0043] A metalloporphyrin **15**, sometimes referred to as M(TPP), of the present invention is depicted in **FIG. 2A**. **FIG. 2A** also depicts various metals of the metalloporphyrins **15** of the present invention, and corresponding metal ion charge to radius ratio (i.e., Z/r Ratio) in reciprocal angstroms. The Z/r Ratio should preferably span a wide range in order to target a wide range of metal ligating analytes. These metalloporphyrins have excellent chemical stability on the solid support and most have well-studied solution ligation chemistry. Reverse phase silica was chosen as a non-interacting dispersion medium for the metalloporphyrin array **16** depicted in FIG. 2B, as well as a suitable surface for diffuse reflectance spectral measurements. More importantly, the reverse phase silica presents a hydrophobic interface, which virtually eliminates interference from ambient water vapor. After spotting, sensor plates **18** like the one depicted in FIG. 2B were dried under vacuum at 50° C. for 1 hour prior to use. Thus, immobilization of the metalloporphyrins on a reverse phase silica support is obtained. While ten (10) different metalloporphyrins are shown in **FIG. 2A**, those of skill in the art will recognize that many other metalloporphyrins are useful in accordance with the present invention. Those of skill in the art will further recognize that in accordance with the broad teachings of the present invention, any dyes capable of changing color upon interacting with an analyte, both containing and not containing metal ions, are useful in the array of the present invention.

[0044] Colorimetric Analysis Using the Sensor Plate

[0045] For the detection and analysis of odorants in accordance with the present invention, one needs to monitor the absorbance of the sensor plate at one or more wavelengths in a spatially resolved fashion. This can be accomplished with an imaging spectrophotometer, a simple flatbed scanner (e.g. a Hewlett Packard Scanjet 3c), or an inexpensive video or CCD camera.

[0046] **FIG. 3A** illustrates a vapor exposure apparatus **19** of the present invention. **FIG. 3B** illustrates top and side views of bottom piece **21** and a top view of top piece **21'** of a vapor exposure flow cell **20** of the present invention. In an embodiment of the present invention for purposes of demonstration, each sensor plate **18** was placed inside of a stainless steel flow cell **20** equipped with a quartz window **22** as shown in **FIGS. 3A and 3B**. Scanning of the sensor plate **18** was done on a commercially available flatbed scanner **24** (Hewlett Packard Scanjet 3c) at 200 dpi resolution, in full color mode. Following an initial scan, a control run with a first pure nitrogen flow stream **26** was performed. The array **16** of plate **18** was then exposed to a second nitrogen flow stream **28** saturated with a liquid analyte **30** of interest. As shown in **FIG. 3A**, the nitrogen flow stream **28** saturated with liquid analyte **30** results in a saturated vapor **32**. Saturated vapor **32**, containing the analyte **30** of interest were generated by flowing nitrogen flow stream **28** at 0.47 L/min. through the neat liquid analyte **30** in a water-jacketed, glass fritted bubbler **34**. Vapor pressures were controlled by regulating the bubbler **34** temperature. As shown in **FIG. 3B**, vapor channels **23** permit vapor flow to sensor plate **18**.

EXAMPLE 1

[0047] Scanning at different time intervals and subtracting the red, green and blue ("RGB") values of the new images from those of the original scan yields a color change profile. This is shown for n-butylamine in FIG. 4, in which color change profiles of the metalloporphyrin sensor array **16** as a function of exposure time to n-butylamine vapor. Subtraction of the initial scan from a scan after 5 min. of N_2 exposure was used as a control, giving a black response, as shown. 9.3% n-butylamine in N_2 was then passed over the array and scans made after exposure for 30 s, 5 min., and 15 min. The red, green and blue ("RGB") mode images were subtracted (absolute value) to produce the color change profiles illustrated. Virtually all porphyrins are saturated after 30 seconds of exposure, yielding a color fingerprint unique for each class of analytes, which is illustrated in FIG. 4.

[0048] More specifically, subtraction of the initial scan **40** from a scan after 5 min. of N_2 exposure was used as a control, giving a black response, as shown in FIG. 4. A nitrogen flow stream containing 0.093% n-butylamine was then passed over the array **16** and scans 42, 44, and 46 were made after exposure for 30 seconds, 5 minutes, and 15 minutes, respectively. The RGB mode images were subtracted (absolute value) using Adobe Photoshop™ (which comprises standard image analyzing software), with contrast enhancement by expanding the pixel range (a 32 value range was expanded to 256 each for the R, G, and B values). Subtraction of exposed and unexposed images gives color change patterns that vary in hue and intensity. Because differentiation is provided by an array of detectors, the system has parallels the mammalian olfactory system. As shown in FIG. 4 and summarized in Table 2 below, the dyes have the following colors in scans 42, 44, and 46.

TABLE 2

(Summarizing Colors of Dyes in FIG. 4, Scans 42, 44, and 46)

Sn^{4+}—No Change	Co^{3+}—Green	Cr^{3+}—Green
Mn^{3+}—No Change	Fe^{3+}—Red	Co^{2+}—Faint Green
Cu^{2+}—No Change	Ru^{2+}—No Change	Zn^{2+}—Light Green
Ag^{2+}—No Change	$2H^{+}$(Free Base "FB")—Light Blue	

[0049] As summarized in Table 3 below, for the TTP array **16** depicted on the left-hand side of FIG. 4, the dyes have the following colors.

TABLE 3

Sn^{4+}—Greenish Yellow	Co^{3+}—Red	Cr^{3+}—Yellow with Dark Red Center
Mn^{3+}—Greenish Yellow	Fe^{3+}—Dark Red	Co^{2+}—Red
Cu^{2+}—Red	Ru^{2+}—Light Yellow	Zn^{2+}—Red
Ag^{2+}—Red	$2H^{+}$ (Free Base "FB")—Red	

EXAMPLE 2

[0050] Visible spectral shifts and absorption intensity differences occur upon ligation of the metal center, leading to readily observable color changes. As is well known to those with skill in the art, the magnitude of spectral shift correlates with the polarizability of the ligand; hence, there exists an electronic basis for analyte distinction. Using metal centers that span a range of chemical hardness and ligand binding affinity, a wide range of volatile analytes (including soft ligands, such as thiols, and harder ligands, such as amines) are differentiable. Because porphyrins have been shown to exhibit wavelength and intensity changes in their absorption bands with varying solvent polarity, it is contemplated that the methods and apparatus of the present invention can be used to colorimetrically distinguish among a series of weakly ligating solvent vapors (e.g., arenes, halocarbons, or ketones), as shown for example in **FIG. 5**.

[0051] A comparison of color changes at saturation for a wide range of analytes is shown in **FIG. 5**. Each analyte is identified under the colored array **16** that identifies each analyte.). DMF stands for the analyte dimethylformamide, and THF stands for the analyte tetrahydrofuran. As shown in **FIG. 5** and summarized in Table 4 below, the colors of each dye in response to a particular analyte are as follows.

TABLE 4

	Analyte: DMF	
Sn^{4+}—No Change	Co^{3+}—Green	Cr^{3+}—No Change
Mn^{3+}—No Change	Fe^{3+}—No Change	Co^{2+}—No Change
Cu^{2+}—Blue	Ru^{2+}—No Change	Zn^{2+}—No Change
Ag^{2+}—No Change	$2H^{+}$ (Free Base "FB")—Blue	
	Analyte: Ethanol	
Sn^{4+}—Dark Blue	Co^{3+}—No Change	Cr^{3+}—Red
Mn^{3+}—No Change	Fe^{3+}—No Change	Co^{2+}—No Change
Cu^{2+}—No Change	Ru^{2+}—No Change	Zn^{2+}—Blue
Ag^{2+}—No Change	$2H^{+}$ (Free Base "FB")—No Change	
	Analyte: Pyridine	
Sn^{4+}—No Change	Co^{3+}—Green	Cr^{3+}—Dark Green
Mn^{3+}—No Change	Fe^{3+}—No Change	Co^{2+}—No Change
Cu^{2+}—No Change	Ru^{2+}—No Change	Zn^{2+}—Green
Ag^{2+}—No Change	$2H^{+}$ (Free Base "FB")—Blue	
	Analyte: Hexylamine	
Sn^{4+}—No Change	Co^{3+}—Dark Green	Cr^{3+}—Green
Mn^{3+}—No Change	Fe^{3+}—Red	Co^{2+}—No Change
Cu^{2+}—Blue	Ru^{2+}—No Change	Zn^{2+}—Green
Ag^{2+}—Dark Blue	$2H^{+}$ (Free Base "FB")—Blue	
	Analyte: Acetonitrile	
Sn^{4+}—Blue	Co^{3+}—Dark Green	Cr^{3+}—No Change
Mn^{3+}—Yellow	Fe^{3+}—Dark Green	Co^{2+}—No Change
Cu^{2+}—Blue	Ru^{2+}—Blue (faint dot)	Zn^{2+}—Blue
Ag^{2+}—No Change	$2H^{+}$ (Free Base "FB")—Blue	
	Analyte: Acetone	
Sn^{4+}—No Change	Co^{3+}—No Change	Cr^{3+}—Red (small dot)
Mn^{3+}—No Change	Fe^{3+}—No Change	Co^{2+}—No Change
Cu^{2+}—Dark Blue	Ru^{2+}—No Change	Zn^{2+}—Dark Blue
Ag^{2+}—No Change	$2H^{+}$ (Free Base "FB")—Blue	
	Analyte: THF	
Sn^{4+}—Dark Blue	Co^{3+}—Green	Cr^{3+}—Red
Mn^{3+}—Blue (small dot)	Fe^{3+}—Dark Green	Co^{2+}—No Change
Cu^{2+}—Blue	Ru^{2+}—No Change	Zn^{2+}—Blue
Ag^{2+}—No Change	$2H^{+}$ (Free Base "FB")—Blue	
	Analyte: CH_2Cl_2	
Sn^{4+}—Dark Blue	Co^{3+}—No Change	Cr^{3+}—No Change
Mn^{3+}—Yellow and Red (small dot)	Fe^{3+}—No Change	Co^{2+}—No Change
Cu^{2+}—Dark Blue	Ru^{2+}—No Change	Zn^{2+}—No Change
Ag^{2+}—No Change	$2H^{+}$ (Free Base "FB")—Blue	
	Analyte: $CHCl_3$	
Sn^{4+}—Dark Blue	Co^{3+}—Dark Green	Cr^{3+}—Yellow (circle)
Mn^{3+}—Yellow	Fe^{3+}—Dark Green (very faint)	Co^{2+}—No Change
Cu^{2+}—Dark Blue (very faint)	Ru^{2+}—No Change	Zn^{2+}—Blue

TABLE 4-continued

Ag^{2+}—Blue (very faint)	$2H^+$ (Free Base "FB")—Blue	
	Analyte: $P(OC_2H_5)_3$	
Sn^{4+}—No Change	Co^{3+}—Yellow	Cr^{30} —Dark Green
Mn^{3+}—No Change	Fe^{3+}—Dark Green (very faint)	Co^{2+}—Greenish Yellow
Cu^{2+}—Dark Blue (faint)	Ru^{2+}—No Change	Zn^{2+}—Greenish Blue
Ag^{2+}—Blue (very faint)	$2H^+$ (Free Base "FB")—Blue	
	Analyte: $P(C_4H_9)_3$	
Sn^{4+}—No Change	Co^{3+}—Yellow and Red	Cr^{3+}—Deep Red
Mn^{3+}—No Change	Fe^{3+}—Dark Green (faint)	Co^{2+}—Red (with some yellow)
Cu^{2+}—No Change	Ru^{2+}—Dark Blue	Zn^{2+}—Yellow
Ag^{2+}—No Change	$2H^+$ (Free Base "FB")—No Change	
	Analyte: $C_6H_{13}SH$	
Sn^{4+}—Green	Co^{3+}—No Change	Cr^{3+}—Yellow circle surrounded by greenish blue circle
Mn^{3+}—Yellow	Fe^{3+}—Dark Green	Co^{2+}—No Change
Cu^{2+}—Dark Blue (faint)	Ru^{2+}—No Change	Zn^{2+}—Green
Ag^{2+}—Blue (very faint)	$2H^+$ (Free Base "FB")—Blue	
	Analyte: $(C_3H_7)_2S$	
Sn^{4+}—Dark Blue (faint)	Co^{3+}—Deep Green	Cr^{3+}—Green
Mn^{3+}—No Change	Fe^{3+}—Dark Green	Co^{2+}—Dark Green (very faint)
Cu^{2+}—Dark Blue (faint)	Ru^{2+}—Green	Zn^{2+}—Green
Ag^{2+}—Blue (very faint)	$2H^+$ (Free Base "FB")—Blue	
	Analyte: Benzene	
Sn^{4+}—No Change	Co^{3+}—Green	Cr^{3+}—Yellow (very faint)
Mn^{3+}—Yellow (some green)	Fe^{3+}—Dark Green	Co^{2+}—No Change
Cu^{2+}—No Change	Ru^{2+}—No Change	Zn^{2+}—Dark Green
Ag^{2+}—No Change	$2H^+$ (Free Base "FB")—Blue	

[0052] The degree of ligand softness (roughly their polarizability) increases from left to right, top to bottom as shown in **FIG. 1**. Each analyte is easily distinguished from the others, and there are family resemblances among chemically similar species (e.g., pyridine and n-hexylamine). Analyte distinction originates both in the metal-specific ligation affinities and in their specific, unique color changes upon ligation. Each analyte was delivered to the array as a nitrogen stream saturated with the analyte vapor at 20° C. (to ensure complete saturation, 30 min. exposures to vapor were used. Although these fingerprints were obtained by exposure to saturated vapors (thousands of ppm), unique patterns can be identified at much lower concentrations.

[0053] The metalloporphyrin array **16** has been used to quantify single analytes and to identify vapor mixtures. Because the images' color channel data (i.e., RGB values) vary linearly with porphyrin concentration, we were able to quantify single porphyrin responses to different analytes. Color channel data were collected for individual spots and plotted, for example, as the quantity $(R_{plt}-R_{spt})/(R_{plt})$, (where R_{plt} was the red channel value for the initial silica surface and R_{spt} the average value for the spot. For example, Fe(TFPP)(Cl) responded linearly to octylamine between 0 and 1.5 ppm. Other porphyrins showed linear response ranges that varied with ligand affinity (i.e., equilibrium constant).

EXAMPLE 3

[0054] The array of the present invention has demonstrated interpretable and reversible responses even to analyte mixtures of strong ligands, such as pyridines and phosphites, as is shown in **FIG. 6**. Color change patterns for the mixtures are distinct from either of the neat vapors. Good reversibility was demonstrated for this analyte pair as the vapor mixtures were cycled between the neat analyte extremes, as shown in **FIG. 6**, which shows the two component saturation responses to mixtures of 2-methylpyridine ("2MEPY") and trimethylphosphite ("TMP"). Vapor mixtures were obtained by mixing the analyte-saturated N_2 streams at variable flow ratios. A single plate was first exposed to pure trimethylphosphite vapor in N_2 (Scan A), followed by increasing mole fractions of 2-methylpyridine up to pure 2-methylpyridine vapor (Scan C), followed by decreasing mole fractions of 2-methylpyridine back to pure trimethylphosphite vapor. In both directions, scans were taken at the same mole fraction trimethylphosphite and showed excellent reversibility; scans at mole fractions at 67% trimethylphosphite (χ_{tmp}=0.67, Scans B and D) and of their difference map are shown (Scan E). Response curves for the individual porphyrins allow for quantification of the mixture composition. The colors of each dye upon exposure to the analytes TMP and 2MEPY are shown in **FIG. 6** and are summarized in Table 5 below.

TABLE 5

	Scan A, Analyte: Neat TMP	
Sn^{4+}—Dark Blue	Co^{3+}—Yellow	Cr^{3+}—No Change
Mn^{3+}—Yellow with red center	Fe^{3+}—Dark Green	Co^{2+}—Greenish Yellow
Cu^{2+}—Dark Blue	Ru^{2+}—No Change	Zn^{2+}—Blue
Ag^{2+}—Green (very faint)	$2H^{+}$ (Free Base "FB")—Reddish Blue	
	Scan B, Analyte: TMP,x_{TMP} = 0.67	
Sn^{4+}—Blue	Co^{3+}—Green	Cr^{3+}—Green (small dot)
Mn^{3+}—Yellow and Green	Fe^{3+}—Green and Yellow	Co^{2+}—Green with red center
Cu^{2+}—Dark Blue	Ru^{2+}—Purple (very faint)	Zn^{2+}—Blue
Ag^{2+}—Greenish Blue	$2H^{+}$ (Free Base "FB")—Reddish Blue	
	Scan C, Analyte: Neat 2MEPY	
Sn^{4+}—Blue	Co^{3+}—Green	Cr^{3+}—No Change
Mn^{3+}—Yellow and Green with Red center	Fe^{3+}—Red with some Yellow	Co^{2+}—Green
Cu^{2+}—Dark Blue	Ru^{2+}—Deep Blue	Zn^{2+}—Green with some Blue
Ag^{2+}—Green with some Blue	$2H^{+}$ (Free Base "FB")—Reddish Blue	
	Scan D, Analyte: TMP,x_{TMP} = 0.67	
Sn^{4+}—Blue	Co^{3+}—Green	Cr^{+}—No Change
Mn^{3+}—Yellow and Green	Fe^{3+}—Green and Yellow	Co^{2+}—Green
Cu^{2+}—Dark Blue	Ru^{2+}—Purple (very faint)	Zn^{2+}—Blue
Ag^{2+}—Greenish Blue (very faint)	$2H^{+}$ (Free Base "FB")—Reddish Blue	
	Scan E	
Sn^{4+}—No Change	Co^{3+}—No Change	Cr^{3+}—No Change
Mn^{3+}—No Change	Fe^{3+}—No Change	Co^{2+}—No Change
Cu^{2+}—Blue (very faint)	Ru^{2+}—Blue (small dot)	Zn^{2+}—No Change
Ag^{2+}—Blue (very faint)	$2H^{+}$ (Free Base "FB")—Green	

[0055] In an effort to understand the origin of the color changes upon vapor exposure, diffuse reflectance spectra were obtained for single porphyrin spots before and after exposure to analyte vapors. Porphyrin solutions were spotted in 50 μL aliquots onto a plate and allowed to dry under vacuum at 50° C. Diffuse reflectance spectra of the plate were then taken using a UV-visible spectrophotometer equipped with an integrating sphere. Unique spectral shifts were observed upon analyte exposure, which correlated well with those seen from solution ligation. For example, Zn(TPP) exposure to ethanol and pyridine gave unique shifts which were very similar to those resulting from ligand exposure in solution. **FIG. 7** shows a comparison of Zn(TPP) spectral shifts upon exposure to ethanol and pyridine (py) in methylene chloride solution (A) and on the reverse phase support (B). In both A and B, the bands correspond, from left to right, to Zn(TPP), Zn(TPP)(C_2H_5OH), and Zn(TPP)(py), respectively. Solution spectra (A) were collected using a Hitachi U-3300 spectrophotometer; Zn(TPP), C_2H_5OH, and py concentrations were approximately 2 μM, 170 mM, and 200 μM, respectively. Diffuse reflectance spectra (B) were obtained with an integrating sphere attachment before exposure to analytes, after exposure to ethanol vapor in N_2, and after exposure to pyridine vapor in N_2 for 30 min. each using the flow cell.

[0056] Improvement to Low Concentration Response

[0057] Color changes at levels as low as 460 ppb have been observed for octylamine vapor, albeit with slow response times due to the high surface area of the silica on the plate **18**. The surface area of C2 plates is ≈350 m^2/gram. Removal of excess silica gel surrounding the porphyrin spots from the plate **18** led to substantial improvements in response time for exposures to trace levels of octylamine. Because the high surface area of the reverse phase silica surface is primarily responsible for the increased response time, other means of solid support or film formation can be used to improve low concentration response.

[0058] Further, the present invention contemplates miniaturization of the array using small wells **60** (<1 mm), for example in glass, quartz, or polymers, to hold metalloporphyrin or other dyes as thin films, which are deposited as a solution, by liquid droplet dispersion (e.g., airbrush or inkjet), or deposited as a solution of polymer with metalloporphyrin.

[0059] These embodiments are depicted in **FIGS. 8, 9**, and **10**. **FIG. 8** illustrates the interfacing of a microplate **60** into an assembly consisting of a CCD **70**, a microplate **72** and a light source **74**. **FIG. 9** illustrates another embodiment of the present invention, and more particularly, a microwell porphyrin array wellplate **80** constructed from polydimethylsiloxane (PDMS). The colors of the dyes shown in **FIG. 9** are summarized below in Table 6.

TABLE 6

Sn^{4+}—Dark Red	Co^{3+}—Dark Red	Cr^{3+}—Dark Green
Mn^{3+}—Green	Fe^{3+}—Dark Red	Co^{2+}—Yellowish Green
Cu^{2+}—Deep Red	Ru^{2+}—Dark Red	Zn^{2+}—Red

TABLE 6-continued

Ag^{2+}—Red	$2H^+$ (Free Base "FB")—Red	with some Yellow

[0060] **FIG. 10** demonstrates deposition of metalloporphyrin/polymer (polystyrene/dibutylphthalate) solutions upon a plate, which includes a series of micro-machined Teflon® posts **100** having the same basic position relative to each other as shown in **FIG. 2**A and FIG. 2B. The colors for the dyes in the middle of **FIG. 10** are summarized in Table 7 below.

TABLE 7

Sn^{4+}—Yellow	Co^{3+}—Orange	Cr^{3+}—Yellow
Mn^{3+}—Yellow	Fe^{3+}—Orange	Co^{2+}—Orange
Cu^{2+}—Orange	Ru^{2+}—Dark Yellow	Zn^{2+}—Orange
Ag^{2+}—Orange	$2H^+$ (Free Base "FB")—Red	

[0061] The colors for the dyes on the right hand side of **FIG. 10** are summarized in Table 8 below.

TABLE 8

Sn^{4+}—No Change	Co^{3+}—Green	Cr^{3+}—Red
Mn^{3+}—Blue	Fe^{3+}—Red	Co^{2+}—Red, Green, Blue, and Yellow
Cu^{2+}—Green with some Blue	Ru^{2+}—Blue (very faint)	Zn^{2+}—Yellow with some Red
Ag^{2+}—Green with some Blue	2H+ (Free Base "FB")—Green with some Blue	

EXAMPLE 5

[0062] **FIG. 11** shows the color profile changes from a microplate of the type shown in **FIG. 10**. The microplate, consisting of a minimized array of four metalloporphyrins, i.e., Sn(TPP)(Cl_2), Co(TPP)(Cl), Zn(TPP), Fe(TFPP)(Cl), clockwise from the upper left (where TFPP stands for 5,10,15,20-tetrakis(pentafluorophenyl)porphyrinate). The color profile changes are shown in **FIG. 11** after exposure to low levels of n-octylamine, dodecanethiol ($C_{12}H_{25}$ SH), and tri-n-butylphosphine ($P(C_4H_9)_3$), each at 1.8 ppm, which is summarized in Table 9 below.

TABLE 9

Dyes on Teflon ®	
Sn—Dark Yellow	Co—Red
Zn—Red	Fe—Orange with Red outline
Dyes exposed to n-octylamine	
Sn—No Change	Co—Green (very faint)
Zn—Red	Fe—Green
Dyes exposed to C_{12} H_{25} SH	
Zn—Red with some green and yellow	Fe—Blue (very faint)

TABLE 9-continued

Dyes exposed to $P(C_4$ $H_9)_3$	
Sn—No Change	Co—Yellow with red center and some red periphery
Zn—Green	Fe—Yellow with some Green and Blue

[0063] The low ppm levels of octylamine, an analyte of interest, were generated from temperature-regulated octylamine/dodecane solutions with the assumption of solution ideality. The dodecane acts as a diluent to lower the level of octylamine vapor pressure for the purposes of this demonstration of the invention.

EXAMPLE 6

[0064] **FIG. 12** illustrates the immunity of the present invention to interference from water vapor. The hydrophobicity of the reverse phase support greatly any possible effects from varying water vapor in the atmosphere to be tested. For instance, as shown in **FIG. 12, a** color fingerprint generated from exposure of the array to n-hexylamine (0.86% in N_2) was identical to that for n-hexylamine spiked heavily with water vapor (1.2% H_2O, 0.48% hexylamine in N_2). See scans 120, 122 and 124. The ability to easily detect species in the presence of a large water background represents a substantial advantage over mass-sensitive sensing techniques or methodologies that employ polar polymers as part of the sensor array. The color patterns shown in **FIG. 12** are summarized in Table 10 below.

TABLE 10

Scan 120		
Sn^{4+}—No Change	Co^{3+}—Green	Cr^{3+}—Green
Mn^{3+}—No Change	Fe^{3+}—Red	Co^{2+}—No Change
Cu^{2+}—No Change	Ru^{2+}—No Change	Zn^{2+}—Green
Ag^{2+}—No Change	$2H^+$ (Free Base "FB")—Dark Blue	
Scan 122		
Sn^{4+}—No Change	Co^{3+}—Green	Cr^{3+}—Green
Mn^{3+}—No Change	Fe^{3+}—Red	Co^{2+}—No Change
Cu^{2+}—No Change	Ru^{2+}—Green (small dot)	Zn^{2+}—Green
Ag^{2+}—No Change	$2H^+$ (Free Base "FB")—Dark Blue	
Scan 124		
Sn^{4+}—Bluish Circle	Co^{3+}—Bluish Circle	Cr^{3+}—Bluish Circle

TABLE 10-continued

Mn^{3+}—Bluish Circle	Fe^{3+}—Bluish Circle	Co^{2+}—Bluish Circle
Cu^{2+}—Bluish Circle	Ru^{2+}—Bluish Circle	Zn^{2+}—Bluish Circle
Ag^{2+}—Bluish Circle	$2H^{+}$ (Free Base "FB")—Bluish Circle	

[0065] Additional Features of the Preferred Embodiments of the Invention

[0066] Having demonstrated electronic differentiation, an important further goal is the shape-selective distinction of analytes (e.g., n-hexylamine vs. cyclohexylamine). Functionalized metalloporphyrins that limit steric access to the metal ion are candidates for such differentiation. For instance, we have been able to control ligation of various nitrogenous ligands to dendrimer-metalloporphyrins and induce selectivities over a range of more than 10^4. As an initial attempt toward shape-selective detection, we employed the slightly-hindered tetrakis(2,4,6-trimethoxyphenyl)porphyrins (TTMPP) in our sensing array. With these porphyrins, fingerprints for t-butylamine and n-butylamine showed subtle distinctions, as did those for cyclohexylamine and n-hexylamine. Using more hindered metalloporphyrins, it is contemplated that the present invention can provide greater visual differentiation. Such porphyrins include those whose periphery is decorated with dendrimer, siloxyl, phenyl, t-butyl and other bulky substituents, providing sterically constrained pockets on at least one face (and preferably both) of the porphyrin.

[0067] In a similar fashion, it is contemplated that the sensor plates of the present invention can be used for the detection of analytes in liquids or solutions, or solids. A device that detects an analyte in a liquid or solution or solid can be referred to as an artificial tongue. Proper choice of the metal complexes and the solid support must preclude their dissolution into the solution to be analyzed. It is preferred that the surface support repel any carrier solvent to promote the detection of trace analytes in solution; for example, for analysis of aqueous solutions, reverse phase silica has advantages as a support since it will not be wetted directly by water.

[0068] Alternative sensors in accordance with the present invention may include any other dyes or metal complexes with intense absorbance in the ultraviolet, visible, or near infrared spectra that show a color change upon exposure to analytes. These alternative sensors include, but are not limited to, a variety of macrocycles and non-macrocycles such as chlorins and chlorophylls, phthalocyanines and metallophthalocyanines, salen-type compounds and their metal complexes, or other metal-containing dyes.

[0069] The present invention can be used to detect a wide variety of analytes regardless of physical form of the analytes. That is, the present invention can be used to detect any vapor emitting substance, including liquid, solid, or gaseous forms, and even when mixed with other vapor emitting substances, such solution mixtures of substances.

[0070] The present invention can be used in combinatorial libraries of metalloporphyrins for shape selective detection of substrates where the substituents on the periphery of the macrocycle or the metal bound by the porphyrin are created and then physically dispersed in two dimensions by (partial) chromatographic or electrophoretic separation.

[0071] The present invention can be used with chiral substituents on the periphery of the macrocycle for identification of chiral substrates, including but not limited to drugs, natural products, blood or bodily fluid components.

[0072] The present invention can be used for analysis of biological entities based on the surface proteins, oligosacharides, antigens, etc., that interact with the metalloporphyrin array sensors of the present invention. Further, the sensors of the present invention can be used for specific recognition of individual species of bacteria or viruses.

[0073] The present invention can be used for analysis of nucleic acid sequences based on sequence specific the surface interactions with the metalloporphyrin array sensors. The sensors of the present invention can be used for specific recognition of individual sequences of nucleic acids. Substituents on the porphyrins that would be particularly useful in this regard are known DNA intercalating molecules and nucleic acid oligomers.

[0074] The present invention can be used with ordinary flat bed scanners, as well as portable miniaturized detectors, such as CCD detectors with microarrays of dyes such as metalloporphyrins.

[0075] The present invention can be used for improved sensitivity, automation of pattern recognition of liquids and solutions, and analysis of biological and biochemical samples.

[0076] Superstructure Bonded to the Periphery of the Porphyrin

[0077] The present invention includes modified porphyrins that have a superstructure bonded to the periphery of the porphyrin. A superstructure bonded to the periphery of the porphyrin in accordance with the present invention includes any additional structural element or chemical structure built at the edge of the porphyrin and bonded thereto.

[0078] The superstructures can include any structural element or chemical structure characterized in having a certain selectivity. Those of skill in the art will recognize that the superstructures of the present invention include structures that are shape selective, polarity selective, inantio selective, regio selective, hydrogen bonding selective, and acid-base selective. These structures can include siloxyl-substituted substituents, nonsiloxyl-substituted substituents and nonsiloxyl-substituted substituents, including but not limited to aryl substituents, alkyl substituents, and organic, organometallic, and inorganic functional group substituents.

[0079] Superstructure Bis-Pocket Porphyrins

[0080] A number of modified porphyrins have been synthesized to mimic various aspects of the enzymatic functions of heme proteins, especially oxygen binding (myoglobin and hemoglobin) and substrate oxidation (cytochrome P-450). See Suslick, K. S.; Reinert, T. J. J. Chem. Ed. 1985, 62, 974; Collman, J. P.; Zhang, X.; Lee, V. J.; Uffelman, E. S.; Brauman, J. I. Science 1993,261, 1404; Collman, J. P.; Zhang, X. in Comprehensive Supramolecular Chemistry; Atwood, J. L.; Davies, J. E. D.; MacNicol, D. D.; Vogtel, F. Eds.; Pergamon: New York, 1996; vol. 5, pp. 1-32; Suslick,

K. S.; van Deusen-Jeffries, S. in Comprehensive Supramolecular Chemistry; Atwood, J. L.; Davies, J. E. D.; MacNicol, D. D.; Vogtel, F. Eds.; Pergamon: New York, 1996; vol. 5, pp. 141-170; Suslick, K. S. in Activation and Functionalization of Alkanes; Hill, C. L., ed.; Wiley & Sons: New York, 1989; pp. 219-241. The notable property of many heme proteins is their remarkable substrate selectivity; the development of highly regioselective synthetic catalysts, however, is still at an early stage. Discrimination of one site on a molecule from another and distinguishing among many similar molecules presents a difficult and important challenge to both industrial and biological chemistry. See Metalloporphyrins in Catalytic Oxidations; Sheldon, R. A. Ed. Marcel Dekker: New York, 1994). Although the axial ligation properties of simple synthetic metalloporphyrins are well documented in literature, see Bampos, N.; Marvaud, V.; Sanders, J. K. M. Chem. Eur. J. 1998, 4, 325; Stibrany, R. T.; Vasudevan, J.; Knapp, S.; Potenza, J. A.; Emge, T.; Schugar, H. J. J. Am. Chem. Soc. 1996, 118, 3980, size and shape control of ligation to peripherally modified metalloporphyrins has been largely unexplored, with few notable exceptions, where only limited selectivities have been observed. See Bhyrappa, P.; Vaijayanthimala, G.; Suslick, K. S. J. Am. Chem. Soc. 1999, 121, 262; Imai, H.; Nakagawa, S.; Kyuno, E. J. Am. Chem. Soc. 1992, 114, 6719.

[0081] The present invention includes the synthesis, characterization and remarkable shape-selective ligation of silylether-metalloporphyrin scaffolds derived from the reaction of 5,10,15,20-tetrakis(2',6'-dihydroxyphenyl)porphyrinatozinc(II) with t-butyldimethylsilyl chloride, whereby the two faces of the Zn(II) porphyrin were protected with six, seven, or eight siloxyl groups. This results in a set of three porphyrins of nearly similar electronics but with different steric encumbrance around central metal atom present in the porphyrin. Ligation to Zn by classes of different sized ligands reveal shape selectivities as large as 10^7.

[0082] A family of siloxyl-substituted bis-pocket porphyrins were prepared according to the scheme of **FIG. 13**. The abbreviations of the porphyrins that can be made in accordance with the scheme shown in **FIG. 13** are as follows:

[0083] Zn(TPP), 5,10,15,20-tetraphenylporphyrinatozinc(II);

[0084] Zn[$(OH)_6$PP], 5-phenyl-10,15,20-tris(2′,6′-dihydroxyphenyl)porphyrinatozinc(II);

[0085] Zn[$(OH)_8$PP], 5,10,15,20-tetrakis(2′,6′-dihydroxyphenyl)porphyrinatozinc(II);

[0086] Zn(Si_6PP), 5(phenyl)-10,15,20-trikis(2′,6′-disilyloxyphenyl)porphyrinatozinc(II);

[0087] Zn(Si_7OHPP), 5,10,15-trikis(2′,6′-disilyloxyphenyl)-20-(2′-hydroxy-6′-silyloxyphenyl)porphyrinatozinc(II);

[0088] Zn(Si_8PP), 5,10,15,20-tetrakis(2′,6′-disilyloxyphenyl)porphyrinatozinc(II). The synthesis of Zn[$(OH)_6$PP], Zn(Si_6PP), and Zn(Si_8PP) is detailed below. Zn[$(OH)_6$PP] and Zn[$(OH)_8$PP] were obtained (see Bhyrappa, P.; Vaijayanthimala, G.; Suslick, K. S. J. Am. Chem. Soc. 1999, 121,262) from demethylation (see Momenteau, M.; Mispelter, J.; Loock, B.; Bisagni, E. J. Chem. Soc. Perkin Trans. 1, 1983, 189) of corresponding free base methoxy compounds followed by zinc(II) insertion. The methoxy porphyrins were synthesized by acid catalysed condensation of pyrrole with respective benzaldehydes following Lindsey procedures. See Lindsey, J. S.; Wagner, R. W. J. Org. Chem. 1989, 54, 828. Metalation was done in methanol with $Zn(O_2CCH_3)_2$. The t-butyldimethylsilyl groups were incorporated into the metalloporphyrin by stirring a DMF solution of hydroxyporphyrin complex with TBDMSiCl (i.e., t-butyldimethylsilyl chloride) in presence of imidazole. See Corey, E. J; Venkateswarlu, A. J. Am. Chem. Soc. 1972, 94, 6190. The octa (Zn(Si_8PP)), hepta (Zn(Si_7OHPP)), and hexa (Zn(Si_6PP)) silylether porphyrins were obtained from Zn[$(OH)_8$PP] and Zn[$(OH)_6$PP], respectively. The compounds were purified by silica gel column chromatography and fully characterized by UV-Visible, ^{1}H-NMR, HPLC, and MALDI-TOF MS.

[0089] The size and shape selectivities of the binding sites of these bis-pocket Zn silylether porphyrins were probed using the axial ligation of various nitrogenous bases of different shapes and sizes in toluene at 25° C. Zn(II) porphyrins were chosen because, in solution, they generally bind only a single axial ligand. Successive addition of ligand to the porphyrin solutions caused a red-shift of the Soret band typical of coordination to zinc porphyrin complexes. There is no evidence from the electronic spectra of these porphyrins for significant distortions of the electronic structure of the porphyrin. The binding constants (K_{eq}) and binding composition (always 1:1) were evaluated using standard procedures. See Collman, J. P.; Brauman, J. I.; Doxsee, K. M.; Halbert, T. R.; Hayes, S. E.; Suslick, K. S. J. Am. Chem. Soc. 1978, 100, 2761; Suslick, K. S.; Fox, M. M.; Reinert, T. J. Am. Chem. Soc. 1984, 106,4522. The K_{eq} values of the silylether porphyrins with nitrogenous bases of different classes are compared with the sterically undemanding Zn(TPP) in **FIGS. 14***a*, **14***b*, and **14***c*. It is worth noting the parallel between shape selectivity in these equilibrium measurements and prior kinetically-controlled epoxidation and hydroxylation. See Collman, J. P.; Zhang, X. in Comprehensive Supramolecular Chemistry; Atwood, J. L.; Davies, J. E. D.; MacNicol, D. D.; Vogtel, F. Eds.; Pergamon: New York, 1996; vol. 5, pp. 1-32; Suslick, K. S.; van Deusen-Jeffries, S. in Comprehensive Supramolecular Chemistry; Atwood, J. L.; Davies, J. E. D.; MacNicol, D. D.; Vogtel, F. Eds.; Pergamon: New York, 1996; vol. 5, pp. 141-170; Suslick, K. S. in Activation and Functionalization of Alkanes; Hill, C. L., ed.; Wiley & Sons: New York, 1989; pp. 219-241; Bhyrappa, P.; Young, J. K.; Moore, J. S.; Suslick, K. S. J. Am. Chem. Soc., 1996, 118, 5708-5711. Suslick, K. S.; Cook, B. R. J. Chem. Soc., Chem. Comm. 1987,200-202; Cook, B. R.; Reinert, T. J.; Suslick, K. S. J. Am. Chem. Soc. 1986, 108, 7281-7286; Suslick, K. S.; Cook, B. R.; Fox, M. M. J. Chem. Soc., Chem. Commun. 1985, 580-582. The selectivity for equilibrated ligation appears to be substantially larger than for irreversible oxidations of similarly shaped substrates.

[0090] The binding constants of silylether porphyrins are remarkably sensitive to the shape and size of the substrates relative to Zn(TPP). See **FIGS. 14***a*, **14***b*, and **14***c*. The binding constants of different amines could be controlled over a range of 10^1 to 10^7 relative to Zn(TPP). It is believed that these selectivities originate from strong steric repulsions

created by the methyl groups of the t-butyldimethylsiloxyl substituents. The steric congestion caused by these bulky silylether groups is pronounced even for linear amines and small cyclic amines (e.g., azetidine and pyrrolidine).

[0091] There are very large differences in K_{eq} for porphyrins having three versus four silylether groups on each face (e.g., hexa- vs. octa-silylether porphyrins), as expected based on obvious steric arguments (see **FIGS. 14*a***, **14*b***, and **14*c***). Even between the hexa- over hepta-silylether porphyrins, however, there are still substantial differences in binding behavior. It is believed that this is probably due to doming of the macrocycle in the hexa- and hepta-silylether porphyrins, which lessens the steric constraint relative to the octasilylether porphyrin. Such doming will be especially important in porphyrins whose two faces are not identical. The free hydroxy functionality of the hepta-silylether may play a role in binding of bi-functionalized ligands (e.g., free amino acids); for the simple amines presented here, however, we have no evidence of any special effects.

[0092] These silylether porphyrins showed remarkable selectivities for normal, linear amines over their cyclic analogues. For a series of linear amines (n-propylamine through n-decylamine), K_{eq} were very similar for each of the silylether porphyrins. In comparison, the relative K_{eq} for linear versus cyclic primary amines (**FIG. 14*a***, n-butylamine vs. cyclohexylamine) were significantly different: $K_{eq}^{linear}/K_{eq}^{cyclic}$ ranges from 1 to 23 to 115 to >200 for Zn(TPP), Zn(Si_6PP), Zn(Si_7OHPP), and Zn(Si_8PP), respectively. The ability to discriminate between linear and cyclic compounds is thus established.

[0093] A series of cyclic 2° amines (**FIG. 14*b***) demonstrate the remarkable size and shape selectivities of this family of bis-pocket porphyrins. Whereas the binding constants to Zn(TPP) with those amines are virtually similar. In contrast, the K_{eq} values for silylether porphyrins strongly depend on the ring size and its peripheral substituents. The effect of these shape-selective binding sites is clear, even for compact aromatic ligands with non-ortho methyl substituents (**FIG. 14*c***).

[0094] The molecular structures of these silylether porphyrins explains their ligation selectivity. The x-ray single crystal structure of Zn(Si_8PP) has been solved in the triclinic P1 bar space group. See Single crystal x-ray structure of Zn(Si_8PP) shown in **FIG. 15**. As shown in **FIG. 15**, Zn(Si_6PP) (energy minimized molecular model) and Zn(Si_8PP) (single crystal x-ray structure) have dramatically different binding pockets. In the octasilylether porphyrin, the top access on both faces of the porphyrin is very tightly controlled by the siloxyl pocket. In contrast, the metal center of the hexasilylether porphyrin is considerably more exposed for ligation.

[0095] **FIG. 15** illustrates molecular models of Zn(Si_6PP) (left column) and Zn(Si_8PP) (right column). The pairs of images from top to bottom are cylinder side-views, side-views, and top-views, respectively; space filling shown at 70% van der Waals radii; with the porphyrin carbon atoms shown in purple, oxygen atoms in red, silicon atoms in green, and Zn in dark red. The x-ray single crystal structure of Zn(Si_8PP) is shown; for Zn(Si_6PP), an energy-minimized structure was obtained using Cerius 2 from MSI.

[0096] In summary, a series of bis-pocket siloxyl metalloporphyrin complexes were prepared with sterically restrictive binding pockets on both faces of the macrocycle. Ligation to Zn by various nitrogenous bases of different sizes and shapes were investigated. Shape selectivities as large as 10^7 were found, compared to unhindered metalloporphyrins. Fine-tuning of ligation properties of these porphyrins was also possible using pockets of varying steric demands. The shape selectivities shown here rival or surpass those of any biological system.

[0097] Examples of Synthesis of Superstructured Porphyrins and Metalloporphyrins

[0098] Synthesis of 5-phenyl-10,15,20-tris(2′,6′-dihydroxy-phenyl)-porphyrinatozinc(II), Zn[$(OH)_6$PP]:

[0099] The free base 5-phenyl-10,15,20-tris(2′,6′-dimethoxyphenyl)-porphyrin was synthesized by Lewis acid catalyzed condensation of 2,6-dimethoxybezaldehyde and benzaldehyde with pyrrole (3:1:4 mole ratio) following the Lindsey procedure. See Lindsey, J. S.; Wagner, R. W. J. Org. Chem. 1989, 54, 828. The mixture of products thus formed was purified by silica gel column chromatography (if necessary, using CH_2Cl_2 as eluant). The isolated yield of the desired product was found to be 7% (wrt pyrrole used). The corresponding hydroxyporphyrins were obtained by demethylation with pyridine hydrochloride. See Momenteau, M.; Mispelter, J.; Loock, B.; Bisagni, E. J. Chem. Soc. Perkin Trans. 1, 1983, 189. After typical work-up known to those skilled in the art, the crude compound was purified by silica gel column chromatography using ethylacetate as eluant. The first fraction was Zn[$(OH)_6$PP], which was collected and the solvent was removed. The yield of the product was 90% (based on starting hydroxyporphryin). ^{1}H NMR of H_2[$(OH)_6$PP] in acetone-d_6 (ppm): 8.96-8.79(m, 8H, b-pyrrole H), 8.24(m, 2H, o-H 5-Phenyl), 8.07 and 8.02(2s, 6H, —OH), 7.83(m, 3H, m,p-H 5-Phenyl), 7.50(t, 3H, p-H hydroxyphenyl), 6.90(d, 6H, m-H hydroxyphenyl), −2.69(s, 2H, imino-H). Elemental analysis, calcd. for $C_{44}H_{30}O_6N_4.H_2O$: C=72.5, H=4.4 and N=7.7%. Found C=72.7, H=4.4 and N=7.4%. The compound showed molecular ion peak at 711 (m/z calcd. for $C_{44}H_{30}O_6N_4$=710) in FAB-MS.

[0100] The Zn derivative was obtain by stirring methanol solution of H_2[$(OH)_6$PP] with excess $Zn(O_2CCH_3)_2 2H_2O$ for 1 hour. Methanol was evaporated to dryness and the residue was dissolved in ethylacetate, washed with water, and the organic layer passed through anhyd. Na_2SO_4. The concentrated ethylacetate solution was passed through a silica gel column and the first band was collected as the desired product. The yield of the product was nearly quantitative. ^{1}H NMR of Zn$(OH)_6$PP in acetone-d_6 (ppm): 8.95-8.79(m, 8H, b-pyrrole H), 8.22(m, 2H, o-H 5-Phenyl), 7.79(m, 3H, m,p-H 5-Phenyl), 7.75 and 7.65(2s, 6H, —OH), 7.48(t, 3H,p-H hydroxyphenyl), 6.88(d, 6H, m-H hydroxyphenyl). Elemental analysis, calcd. for $ZnC_{44}H_{28}O_6N_4.H_2O$: C=66.7, H=3.8, N=7.1 and Zn=8.3%. Found C=66.4, H=3.8, N=6.7 and Zn=8.2%. The compound showed molecular ion peak at 774 (m/z calcd. for $ZnC_{44}H_{28}O_6N_4$=773) in FAB-MS.

[0101] Synthesis of 5-phenyl-10,15,20-tris(2′,6′-disilyloxyphenyl)-porphyrinatozinc(II), Zn(Si_6PP):

[0102] The hexasilylether porphyrin was synthesized by stirring a DMF solution of 5-phenyl-10,15,20-tris(2′,6′-dihydroxyphenyl)-porphyrinatozinc(II) (100 mg, 0.13 mmol)

with t-butyldimethyl silylchloride (1.18 g, 7.8 mmol) in presence of imidazole (1.2 g, 17.9 mmol) at 60° C. for 24 h under nitrogen. After this period the reaction mixture was washed with water and extracted in $CHCl_3$. The organic layer was dried over anhyd. Na_2SO_4. The crude reaction mixture was loaded on a short silica gel column and eluted with mixture of $CHCl_3$/petether (1:1, v/v) to get rid of unreacted starting material and lower silylated products. The desired compound was further purified by running another silica gel column chromatography using mixture of $CHCl_3$/petether (1:3, v/v) as eluant. The yield of the product was 60% based on starting hydroxyporphyrin.

[0103] ^{1}H NMR in chloroform-d (ppm): 8.94-8.82(m, 8H, b-pyrrole H), 8.20(m, 2H, o-H 5-Phenyl), 7.74(m, 3H, m,p-H 5-Phenyl), 7.49(t, 3H, p-H hydroxyphenyl), 6.91(t, 6H, m-H hydroxyphenyl), −0.02 and −0.34(2s, 54H, t-butyl H), −0.43, −0.78 and −1.01(3s, 36H, methyl H). Elemental analysis, calcd. for $ZnC_{80}H_{112}O_6N_4Si_6$: C=65.8, H=7.7, N=3.8, Si=11.5 and Zn=4.5%. Found C=65.5, H=7.7, N=3.8, Si=11.2 and Zn=4.4%. The low resolution MALDI-TOF mass spectrum showed molecular ion peak at 1457 (m/z calcd. for $ZnC_{80}H_{112}O_6N_4Si_6$=1458).

[0104] Synthesis of 5,10,15-tris(2′,6′-disilyoxyphenyl)-20-(2′6′-hydr-oxy-6′-silyloxyphenyl)porphyrinatozinc(II), [Zn(Si_7OHPP)], and 5,10,15,20-tetrakis(2′,6′-disilyloxyphenyl)porphy-rinato-zinc(II), [Zn(Si_8PP)]:

[0105] The synthesis of precursor porphyrin 5,10,15,20-tetrakis-(2′,6′-dihydroxyphenyl)porphyrin and its Zn derivative was accomplished as reported earlier. See Bhyrappa, P.; Vaijayanthimala, G.; Suslick, K. S. J. Am. Chem. Soc. 1999, 121, 262. The hepta-and octa-silylether porphyrins were synthesized by stirring DMF solution of 5,10,15,20-tetrakis(2′,6′-dihydroxyphenyl)porphyrinatozinc(II) (100 mg, 0.12 mmol) with t-butyldimethyl silylchloride (1.45 g, 9.6 mmol) in presence of imidazole (1.50 g, 22.1 mmol) at 60° C. for 24 h under nitrogen. After usual work-up the mixture of crude products were loaded on a silica gel column and eluted with mixture of $CHCl_3$/pet. ether (1:1, v/v) to remove unreacted starting material and lower silylated products. The major product isolated from this column is a mixture of hepta- and octa-silylated porphyrins. The mixture thus obtained was further purified by another silica gel column chromatography using mixture of $CHCl_3$/pet. ether (1:3, v/v) as eluant. The first two bands were isolated as octa- and hepta-silylether porphyrin at 45% and 30% yield, respectively. Both the compounds were characterized by UV-Visible, ^{1}H NMR and MALDI-TOF spectroscopic techniques. The homogeneity of the sample was verified by HPLC.

[0106] For Zn(Si_7OHPP), ^{1}H NMR in chloroform-d (ppm): 8.91(m, 8H, b-pyrrole H), 7.50(m, 4H, p-H), 7.01-6.81(m, 8H, m-H), 0.11 to −0.03(12s, 105H, t-butyl and methyl H). Elemental analysis, calcd. for $ZnC_{86}H_{126}O_8N_4Si_7$: C=64.3, H=7.8, N=3.5, Si=12.3 and Zn=4.1%. Found C=63.6, H=8.1, N=3.5, Si=12.1 and Zn=3.9%. The low resolution MALDI-TOF mass spectrum showed molecular ion peak at 1604 (m/z calcd. for $ZnC_{86}H_{126}O_8N_4Si_7$=1604).

[0107] For Zn(Si_8PP), ^{1}H NMR in chloroform-d (ppm): 8.89(s,8H, b-pyrrole H), 7.49(t, 4H, p-H), 6.92(d,8H, m-H), 0.09(s, 72H, t-butyl H), −1.01(s, 48H, methyl H). Elemental analysis, calcd. for $ZnC_{92}H_{140}O_8N_4Si_8$: C=64.2, H=8.1,N=3.3, Si=13.1 and Zn=3.8%. Found C=63.5, H =8.4, N=3.3, Si=12.8 and Zn=4.0%. The low resolution MALDI-TOF mass spectrum showed molecular ion peak at 1719 (m/z calcd. for $ZnC_{92}H_{140}O_8N_4Si_8$=1718).

[0108] Many modifications and variations may be made in the techniques and structures described and illustrated herein without departing from the spirit and scope of the present invention. Accordingly, the techniques and structures described and illustrated herein should be understood to be illustrative only and not limiting upon the scope of the present invention.

What is claimed is:

1. An artificial nose comprising an array, the array comprising at least a first dye and a second dye in combination and having a distinct spectral response to an analyte wherein the first dye or the second dye are porphyrins each having a periphery and wherein at least the first porphyrin or the second porphyrin has a superstructure bonded to the respective periphery thereof.

2. The artificial nose of claim 1 wherein the superstructure is from the group comprising siloxyl-substituted substituents and nonsiloxyl-substituted substituents, including aryl substituents, alkyl substituents, and organic, organometallic, and inorganic functional group substituents.

3. The artificial nose of claim 1 wherein the superstructure is shape selective, polarity selective, inantio selective, regio selective, hydrogen bonding selective, or acid-base selective.

4. The artificial nose of claim 1 wherein either the first porphyrin or the second porphyrin is a siloxyl-substituted bis-pocket porphyrin.

5. The artificial nose of claim 4 wherein the siloxyl-substituted bis-pocket porphyrin is made in accordance with the synthesis shown in **FIG. 13**.

6. The artificial nose of claim 4 wherein the siloxyl-substituted bis-pocket porphyrin is from the group consisting of Zn(TPP), 5,10,15,20-tetraphenylporphyrinatozinc(II);

Zn[$(OH)_6$PP], 5-phenyl-10, 15,20-tris(2′,6′-dihydroxyphenyl)porphyrinatozinc(II);

Zn[$(OH)_8$PP], 5,10,15,20-tetrakis(2′,6′-dihydroxyphenyl)porphyrinatozinc(II);

Zn(Si_6PP), 5(phenyl)-10,15,20-trikis(2′,6′-disilyloxyphenyl)porphyrinatozinc(II);

Zn(Si_7OHPP), 5,10,15-trikis(2′,6′-disilyloxyphenyl)-20-(2′-hydroxy-6′-silyloxyphenyl)porphyrinatozinc(II); and Zn(Si_8PP), 5,10,15,20-tetrakis(2′,6′-disilyloxyphenyl)porphyrinatozinc(II).

7. The artificial nose of claim 1 wherein the array is part of a sensor plate.

8. The artificial nose of claim 1 wherein the array is connected to a wavelength sensitive light detecting device.

9. The artificial nose of claim 8 wherein the wavelength sensitive light detecting device comprises a scanner.

10. The artificial nose of claim 8 wherein the wavelength sensitive light detecting device comprises a charge-coupled device.

11. The artificial nose of claim 1 wherein the array is a spatially resolved collection of dyes.

12. The artificial nose of claim 1 wherein the array is a spatially resolved combinatorial family of dyes.

13. A method of detecting an analyte comprising the steps of forming an array of at least a first dye and a second dye in combination, subjecting the array to an analyte, and inspecting the first dye and the second dye for a spectral response corresponding to the analyte wherein the first dye or the second dye are porphyrins each having a periphery and wherein at least the first porphyrin or the second porphyrin has a superstructure bonded to the respective periphery thereof.

14. The method of claim 13 wherein the superstructure is from the group comprising siloxyl-substituted substituents and nonsiloxyl-substituted substituents, including aryl substituents, alkyl substituents, and organic, organometallic, and inorganic functional group substituents.

15. The method of claim 13 wherein the superstructure is shape selective, polarity selective, inantio selective, regio selective, hydrogen bonding selective, or acid-base selective.

16. The method of claim 13 wherein either the first porphyrin or the second porphyrin is a siloxyl-substituted bis-pocket porphyrin.

17. The method of claim 16 wherein the siloxyl-substituted bis-pocket porphyrin is made in accordance with the synthesis shown in **FIG. 13**.

18. The method of claim 13 wherein the siloxyl-substituted bis-pocket porphyrin is from the group consisting of Zn(TPP), 5,10,15,20-tetraphenylporphyrinatozinc(II);

Zn[$(OH)_6$PP], 5-phenyl-10,15,20-tris(2′,6′-dihydroxyphenyl)porphyrinatozinc(II);

Zn[$(OH)_8$PP], 5,10,15,20-tetrakis(2′,6′-dihydroxyphenyl)porphyrinatozinc(II);

Zn(Si_6PP), 5(phenyl)-10,15,20-trikis(2′,6′-disilyloxyphenyl)porphyrinatozinc(II);

Zn(Si_7OHPP), 5,10,15-trikis(2′,6′-disilyloxyphenyl)-20-(2′-hydroxy-6′-silyloxyphenyl)porphyrinatozinc(II); and Zn(Si_8PP), 5,10,15,20-tetrakis(2′,6′-disilyloxyphenyl)porphyrinatozinc(II).

19. The method of claim 13 having the step of placing the array on a sensor plate.

20. The method of claim 13 having the step of connecting the array to a visual display or detection device.

21. The method of claim 20 wherein the wavelength sensitive light detecting device comprises a scanner.

22. The method of claim 20 wherein the wavelength sensitive light detecting device comprises a charge-coupled device.

23. The method of claim 13 wherein the array is a spatially resolved collection of dyes.

24. The method of claim 13 wherein the array is a spatially resolved combinatorial family of dyes.

25. The method of claim 13 having the further step of comparing the spectral response with a catalog of analyte spectral responses to identify the analyte.

26. An artificial tongue comprising an array, the array comprising at least a first dye and a second dye in combination and having a distinct spectral response to an analyte in solution or a liquid analyte, or an analyte in a solid or a solid analyte, wherein the first dye or the second dye are porphyrins each having a periphery and wherein at least the first porphyrin or the second porphyrin has a superstructure bonded to the respective periphery thereof.

27. The artificial tongue of claim 26 wherein the superstructure is from the group comprising siloxyl-substituted substituents and nonsiloxyl-substituted substituents, including aryl substituents, alkyl substituents, and organic, organometallic, and inorganic functional group substituents.

28. The artificial tongue of claim 26 wherein the superstructure is shape selective, polarity selective, inantio selective, regio selective, hydrogen bonding selective, or acid-base selective.

29. The artificial tongue of claim 26 wherein either the first porphyrin or the second porphyrin is a siloxyl-substituted bis-pocket porphyrin.

30. The artificial tongue of claim 29 wherein the siloxyl-substituted bis-pocket porphyrin is made in accordance with the synthesis shown in **FIG. 13**.

31. The artificial tongue of claim 29 wherein the siloxyl-substituted bis-pocket porphyrin is from the group consisting of Zn(TPP), 5,10,15,20-tetraphenylporphyrinatozinc(II);

Zn[$(OH)_6$PP], 5-phenyl-10,15,20-tris(2′,6′-dihydroxyphenyl)porphyrinatozinc(II);

Zn[$(OH)_8$PP], 5,10,15,20-tetrakis(2′,6′-dihydroxyphenyl)porphyrinatozinc(II);

Zn(Si_6PP), 5(phenyl)-10,15,20-trikis(2′,6′-disilyloxyphenyl)porphyrinatozinc(II);

Zn(Si_7OHPP), 5,10,15-trikis(2′,6′-disilyloxyphenyl)-20-(2′-hydroxy-6′-silyloxyphenyl)porphyrinatozinc(II); and Zn(Si_8PP), 5,10,15,20-tetrakis(2′,6′-disilyloxyphenyl)porphyrinatozinc(II).

32. The artificial tongue of claim 26 wherein the array is part of a sensor plate.

33. The artificial tongue of claim 26 wherein the array is connected to a wavelength sensitive light detecting device.

34. The artificial tongue of claim 33 wherein the wavelength sensitive light detecting device comprises a scanner.

35. The artificial tongue of claim 33 wherein the wavelength sensitive light detecting device comprises a charge-coupled device.

36. The artificial tongue of claim 26 wherein the array is a spatially resolved collection of dyes.

37. The artificial tongue of claim 26 wherein the array is a spatially resolved combinatorial family of dyes.

38. A porphyrin having the chemical formula Zn[$(OH)_6$PP], 5-phenyl-10,15,20-tris(2′,6′-dihydroxy-phenyl)-porphyrinatozinc(II).

39. A porphyrin having the chemical formula Zn(Si_6PP), 5-phenyl-10,15,20-tris(2′,6′-disilyloxyphenyl)-porphyrinatozinc(II).

40. A porphyrin having the chemical formula Zn(Si_7OHPP), 5,10,15-tris(2′,6′-disilyoxyphenyl)-20-(2′6′-hydr-oxy-6′-silyloxyphenyl)porphyrinatozinc(II).

41. A porphyrin having the chemical formula Zn(Si_8PP), 5,10,15,20-tetrakis(2′,6′-disilyloxyphenyl)porphy-rinatozinc(II).

* * * * *